

**Characterization and Identification of Antioxidant and
Immunomodulatory Activities of Polysaccharides
Extracted from *Helicteres angustifolia* L.**

July 2018

SUN SHUANG

**Characterization and Identification of Antioxidant and
Immunomodulatory Activities of Polysaccharides
Extracted from *Helicteres angustifolia* L.**

A Dissertation Submitted to
the Graduate School of Life and Environmental Sciences,
University of Tsukuba
in Partial Fulfillment of the Requirements
for the Degree of Doctor of Philosophy in Environmental Studies
(Doctoral Program in Sustainable Environmental Studies)

SUN SHUANG

Abstract

Helicteres angustifolia L. (*H. angustifolia*), a traditional medicinal plant, is widely distributed in China, Laos, and Japan. It has long been used as a remedy against various types of illness relating to oxidation and immune response, such as diabetes, inflammations and fever. Previous works mainly focused on the isolation, determination and bioactivities identification of quinones, triterpenoids, lignins, and alkaloids from this plant. Up to the present, however, limited information is available on the characterization, and identification of antioxidant and immunomodulatory activity of its polysaccharides.

In this study, the *in vivo* immune enhancement ability of crude polysaccharide from *H. angustifolia* (HACP) was identified by using 4T1 breast tumor BALB/c mice. The major bioactive fractions of HACP were then purified stepwise successfully with DEAE Sepharose Fast Flow and Sephacry S-400 chromatography. The primary structure features and molecular weight of the obtained fractions were determined. Moreover, *in vitro* antioxidant and macrophage activation abilities were also evaluated.

After orally administering HACP to 4T1 tumor-bearing mice for continuous 15 days, the mice immune response was found significantly ($p < 0.05$) improved. Especially, 300 mg/kg of HACP treatment increased mouse spleen indices, CD4⁺ and CD8⁺ ratios about 1.9, 2.0, and 1.4 times compared to the tumor control group. The increased immune response resulted in a reduced tumor weight and lung metastasis, with inhibition rates of 67.7% and 13.7%, respectively. Three major bioactive fractions were then fractionated and purified from HACP, yielding 7.4%, 6.9% and 9.8% of the total amount of HACP, respectively. Physicochemical analysis demonstrates that SPF1-1, SPF2-1, and SPF3-1 are typical pectic polysaccharides which have different molecular weights and structure features.

Among the three SPF fractions, significant high arabinose and relative higher galactose and xylose levels were detected in SPF3-1, highly correlating with DPPH radical inhibition effect, reducing power and metal chelating activity. *In vitro* immunomodulatory assay demonstrates that the fraction SPF3-1 with the highest uronic acid content (58.8%) and lowest molecular weight (13.36 kD) has been proven to possess the highest immunomodulatory activities, this observation is attributable to the significant ($p < 0.05$) proliferation and phagocytic capacity of macrophage cells. In addition, remarkably releases of IL-6 and TNF- α were detected in SPF3-1 treated cells in a dose-dependent manner. Furthermore, SPF3-1 was found to possess obvious induction

effect on lymphocytes proliferation, with the highest viability increased to 196% after 100 µg/mL of SPF3-1 treatment for 48 h, indicating its potent lymphocyte activation function. Moreover, 100 µg/mL of SPF3-1 treatment efficiently promoted lymphocytes IL-6 and IFN-γ release (117.3 and 63.6 pg/mL), significantly higher than the control groups (36.8 pg/mL and 21.0 pg/mL).

In conclusion, HACP from *H. angustifolia* exhibit potent antioxidant and immunomodulatory activity *in vivo*. Fraction SPF3-1 with higher antioxidant and macrophages activation abilities could be further developed as new products for medicines or functional foods.

Keywords: Antioxidant; Immunomodulatory; *Helicteres angustifolia* L.; Polysaccharide

Contents

Abstract.....	I
Contents.....	III
List of Tables.....	VI
List of Figures.....	VII
Chapter 1 Introduction.....	1
1.1. Polysaccharide.....	1
1.1.1. The structure of polysaccharide.....	1
1.1.2. Bioactive polysaccharides in herbs.....	1
1.1.3. The antioxidant and immunomodulatory activities of polysaccharides...	1
1.2. <i>Helicteres angustifolia</i> L.....	3
1.2.1. Phytochemical composition of <i>H. angustifolia</i>	3
1.2.2. Pharmacological activity of <i>H. angustifolia</i>	3
1.3. Target and structure of the thesis.....	4
Chapter 2 Immunomodulatory activity of polysaccharides from <i>H. angustifolia</i> against breast cancer.....	10
2.1. Introduction.....	10
2.2. Materials and methods.....	10
2.2.1. Plant material and chemicals.....	10
2.2.2. Polysaccharide extraction.....	11
2.2.3. Determination of chemical composition.....	11
2.2.4. Cell culture.....	11
2.2.5. Cytotoxicity effect on 4T1 cells.....	11
2.2.6. Sub-acute toxicity study.....	11
2.2.7. Design for mouse experiment.....	12
2.2.8. Histopathology staining.....	12
2.2.9. Determination of spleen lymphocyte phenotype.....	13
2.2.10. Antioxidant enzyme activities and cytokines production in mice seru..	13
2.2.11. Splenocytes proliferation and natural killer (NK) cell activity.....	13
2.2.12. Statistical analysis.....	14
2.3. Results and discussion.....	14
2.3.1. Chemical composition of HACP.....	14
2.3.2. Non-toxicity of HACP on 4T1 cells <i>in vitro</i>	14

2.3.3.	HACP does not show any acute toxicity <i>in vivo</i>	14
2.3.4.	HACP inhibited tumor growth in 4T1 cell-bearing mice.....	14
2.3.5.	HACP inhibited 4T1 mammary metastasis to lung.....	15
2.3.6.	HACP induced apoptosis and angiogenesis reduction in tumors.....	15
2.3.7.	HACP increased the immune organ indices, as well as CD4 ⁺ /CD8 ⁺ ratios in spleen lymphocyte.....	15
2.3.8.	HACP regulated the antioxidant enzymes and cytokines production in serum of tumor-bearing mice.....	15
2.3.9.	Effect of HACP on splenocytes proliferation and NK cell activity.....	16
2.4.	Discussion.....	16
2.5.	Summary.....	18
Chapter 3 Purification and characterization of polysaccharide fractions from HACP.....		28
3.1.	Introduction.....	28
3.2.	Materials and methods.....	28
3.2.1.	Chemicals and reagents.....	28
3.2.2.	Purification of HACP.....	28
3.2.3.	Chemical composition and molecular weight (Mw).....	29
3.2.4.	FTIR and UV spectroscopy.....	30
3.2.5.	Nuclear magnetic resonance (NMR) analysis.....	30
3.2.6.	SEM analysis.....	30
3.3.	Results and discussion.....	30
3.3.1.	Purification and separation of HACP.....	30
3.3.2.	Monosaccharide composition and molecular weight.....	31
3.3.3.	UV and FT-IR spectra analysis.....	31
3.3.4.	NMR analysis.....	31
3.3.5.	SEM analysis.....	32
3.4.	Discussion.....	32
3.5.	Summary.....	33
Chapter 4 <i>In vitro</i> antioxidant and immunomodulatory effects of polysaccharide fractions		42
4.1.	Introduction.....	42
4.2.	Materials and methods.....	42
4.2.1.	Chemicals and reagents.....	42

4.2.2. Antioxidant activity assays.....	43
4.2.3. Cell line and culture.....	45
4.2.4. Cytotoxicity of SPF3-1.....	45
4.2.5. <i>In vitro</i> immunomodulatory activities.....	45
4.2.6. Statistical analysis.....	47
4.3. Results and discussion.....	47
4.3.1. <i>In vitro</i> antioxidant activities.....	47
4.3.2. <i>In vitro</i> immunomodulatory activities.....	49
4.4. Discussion.....	51
4.5. Summary.....	53
Chapter 5 Conclusions and perspectives.....	63
5.1. Conclusions.....	63
5.2. Future researches.....	63
References.....	66
Acknowledgements.....	75

List of tables

Table 1- 1 Polysaccharide drugs and healthy products of commercially available.....	6
Table 1-2 Phytochemical composition of <i>H. angustifolia</i>	7
Table 2- 1 Effects of HACP on immune organ indices, and T cell subsets in the spleen of tumor bearing mice.....	19
Table 3- 1 Chemical composition and molecular weight of SPF1-1, SPF2-1, and SPF3-1 错误! 未定义书签。	
Table 4-1 Macrophage cell proliferation ability (%) of polysaccharide fractions from HACP.....	54

List of figures

Figure 1-1 <i>H. angustifolia</i> used in this study.....	8
Figure 1-2 Number of papers with the topics “polysaccharides and immunostimulatory”.	9
Figure 2-1 <i>In vitro</i> cytotoxic effect of HACP on 4T1 breast tumor cells.....	20
Figure 2-2 Inhibition effects of HACP on 4T1 tumor growth.....	21
Figure 2-3 Inhibition effects of HACP on 4T1 tumor metastasis to lung.....	22
Figure 2-4 H&E staining and CD34 immunochemistry of tumor tissues from 4T1 tumor-bearing mice.....	23
Figure 2-5 Cytokine production in mice serum.....	24
Figure 2-6 Antioxidant enzyme levels in the serum of 4T1 tumor-bearing mice.....	25
Figure 2-7 Effect of HACP on the NK cell activity of 4T1 tumor-bearing mice.....	26
Figure 2-8 Effect of HACP on splenocytes proliferation of 4T1 tumor-bearing mice.....	27
Figure 3-1 Purification and characterization of polysaccharide fractions from HACP.....	36
Figure 3-2 UV spectrum of polysaccharide fractions.....	38
Figure 3-3 FTIR spectrum of polysaccharide fractions.....	39
Figure 3-4 ¹ H NMR spectrum of polysaccharide fractions.....	40
Figure 3-5 SEM analysis of polysaccharide fractions SPF1-1, SPF2-1, and SPF3-1.....	41
Figure 4-1 Antioxidant activities of polysaccharide fractions separated from HACP.....	56
Figure 4-2 Activation effects of SPFs on RAW264.7 cells.....	57
Figure 4-3 Production of cytokines of macrophage cells treated by SPF3-1.....	59
Figure 4-4 SPF3-1 induced cytotoxicity of macrophages against HT1080 tumor cells....	60
Figure 4-5 Effect of SPF3-1 on splenocytes proliferation of 4T1-bearing mice.....	61
Figure4-6 Effects of SPF3-1 on cytokines production in the culture medium of spleen lymphocytes.....	62

Chapter 1 Introduction

1.1. Polysaccharide

Polysaccharide is a kind of polymeric carbohydrates consisting more than ten of monosaccharides linked by glycosidic bonds. Being widely existed in plants, animals, algae, and microorganisms, play important roles in cell adhesion, cell-cell communication, and molecular recognition (Yu et al., 2018).

1.1.1. The structure of polysaccharide

Based on the numbers of monosaccharide types present in the molecule, the polysaccharides are classified into two types, homo-polysaccharides (homoglycans) and hetero-polysaccharides (heteroglycans). Homoglycans are polysaccharides which consist of a single type of monosaccharide, such as cellulose (Liu, Willfor, & Xu, 2015). On the other hand, polysaccharides such as hyaluronic acid, which made up of more than one type of monosaccharide are called heteroglycans. According to the glycosides linked onto the glycan, polysaccharides can also be classified as glycoproteins, glycolipids, proteoglycans, and glycoconjugates (Berg, Tymoczko, & Stryer, 2012).

Unlike other biopolymers, polysaccharides can exist in both a linear structural form and branched forms. The structural type of a polysaccharide largely determines its physicochemical properties, particularly solubility in water. Regular linear polysaccharides, such as cellulose, are insoluble in water since the energy of molecular interaction is greater than the hydration energy. Highly branched polysaccharides that do not have an ordered structure are readily soluble in water.

1.1.2. Bioactive polysaccharides in herbs

In traditional Chinese medicines, herbs have been used to treat various types of illness. It has been identified as one of the major active ingredients responsible for various pharmacological activities, such as immunomodulatory activity, antiviral activity, antioxidant activity, antitumor activity, hepatoprotection effect, and antifatigue effect (Harlev, Nevo, Lansky, Ofir, & Bishayee, 2012; Jin, Huang, Zhao, & Shang, 2013; Li & Peng, 2013; Tian, Zhao, Guo, & Yang, 2011; Tang, Hemm, & Bertram, 2003a). According to China Food and Drug Administration (CFDA), there are 38 kinds of drugs and 85 kinds of healthcare products are composed of polysaccharides. Some specific drugs and products are summarized in Table 1-1.

1.1.3. The antioxidant and immunomodulatory activities of polysaccharides

In recent years, polysaccharides from natural sources have attracted increasing attention due to their wide variety of pharmacological activities and non-toxic properties (Huang, Zhao, & Shang, 2013; Liu et al., 2018; Meng et al., 2016; Nie et al., 2018;). Specifically, pectic polysaccharide, and galactomannan isolated from higher plant have been all proved to possess antioxidant and immunomodulatory activities (Di et al., 2017; Wang et al., 2013; Yu et al., 2018)

Immunomodulation is one of the important defense properties for body preventing infections, inflammatory diseases, and cancer (Yu et al., 2018). The first report related to polysaccharides with immune activity were those antigenic polysaccharides from bacteria (Morgan, 1936). After these, polysaccharides from plants, animals, and algae with less toxic were progressively studied (Ramberg et al., 2010; Schepetkin & Quin, 2006). Nowadays, immunomodulatory polysaccharides from natural resources has been the hot topic of research. Pectic polysaccharides, glucans, arabinogalactans, and xylans are the most studied polysaccharides concerning their possible immunomodulatory activity (Fig. 1-2). It is reported that sulfated polysaccharide obtained from *Cyclocarya paiurus* significantly enhanced the TNF- α and IL-6 cytokines production in macrophages in a dose-dependent manner (Yu et al., 2017). *Juniperus scopolorum* cones polysaccharide was found to direct stimulate NO generation *via* induction of NO synthase (Schepetkin et al., 2005). A study published by Jin et al. (2008) also state that sulfated *Achyranthes bidentata* polysaccharides can increase the proliferation of splenic lymphocytes in a concentration dependent manner, enhance the levels of cytokines IL-2 and TNF- α as well.

As it is well known, increased free radicals in the body will lead to T cell damage, and decreased immune function. Therefore, discovery and evaluation of substance with antioxidant properties have been paid more and more attention in biology and medicine. Studies have found that some polysaccharides derived from higher plant can inhibit lipid peroxidation, enhance the body's ability to scavenge free radicals, and inhibition of oxidation disease (Wang et al., 2017). For example, *Algal* polysaccharides have been demonstrated to play an important role in preventing the oxidative damage in living organisms (Cristina Diaz et al., 2017). Three polysaccharides (GLP-H, GLP-V and GLP-F) isolated from *Ganoderma lucidum* showed the stronger radical scavenging activities and was proved that exhibited antioxidant activities *in vitro* (Fan, Li, Deng, & Ai, 2012). Further, administration of litchi pulp polysaccharide (50-200 mg/kg/d) was found to remarkably enhanced the total antioxidant capacity, as well as superoxidase dismutase

activity in the serum and liver of cyclophosphamide-induced mice (Huang et al., 2016).

1.2. *Helicteres angustifolia* L.

Helicteres angustifolia L. (*H. angustifolia*) (Fig.1-1), with brown color and bitter taste, belonging to the family Sterculiaceae, is a traditional medicinal herb widely distributed in southern China, Laos, and Japan. So far, this plant has been widely used as a remedy against various types of illness, such as cold, headache, inflammations and fever in China (Chang et al., 2001) and diabetes treatment in Laos.

1.2.1. Phytochemical composition of *H. angustifolia*

Previous phytochemical research of this plant has been focused on isolation, analysis or determination of quinones, triterpenoids (Chen et al., 1990; Pan et al., 2008), lignans, flavonoids, and alkaloids (Wang et al., 2012). In a previous study reported by Wang & Liu (1987), dried roots of *H. angustifolia* were extracted with EtOH, after that, the EtOAc-soluble portion was packed on the top of a silica gel column. A new naphthoquinone named helicquinone was then isolated from this fraction, and its structure was found to be 2,3-dihydro-8-hydroxy-3,5,6-trimethynaphtho (2,3-b) furan-4,9-dione on the basis of spectroscopic evidence. Chen et al (1990) isolated four sesquiterpenoid quinones from the root bark of *H. angustifolia* which were identified as mansonones E, F, H, and M. In 2001, three lupine type triterpenoids, methyl helicterate, 3-acetoxy-27-benzoyloxylup-20(29)-en-28-oic acid, and 3 β -acetoxy-27-(*p*-hydroxyl) benzoyloxylup-20(29)-en-28-oic acid methyl ester were isolated from the CH₂Cl₂ fraction of the MeOH extracts of *H. angustifolia* root. In addition, four new compounds, including 2 α , 7 β , 20 α -Trihydroxy-3 β , 21-dimethoxy-5-pregnene (1), 6, 7, 9 α -trihydroxy-3, 8, 11 α -trimethylcyclohexo-[d, e]-coumarin (2), 3 β -hydroxy-27-benzoyloxylup-20(29)-en-28-oic acid (3), and 3 β -hydroxy-27-benzoyloxylup-20(29)-en-28-oic acid methyl ester (4) along with other 24 known compounds (including triterpenoids, lignans and phenolic compounds) were isolated and structure characterized from roots of *H. angustifolia* (Chen et al., 2006). Most recently, along with thirteen known compounds, Wang et al. (2012) isolated two new pregnane derivatives, heligenin A-B, and a new quinolone alkaloid (helicterine A) from the ethanol extract of the root of *H. angustifolia* (Table 1-2).

1.2.2. Pharmacological activity of *H. angustifolia*

Various traditional uses of *H. angustifolia* have lead researchers to investigate its bioactivities. Several pharmacological activities have been reported to be exhibited by

extracts as well as single compounds of *H. angustifolia*, such as antioxidant, antiviral, anti-diabetic, and anticancer. In 2008, Pan et al. reported three triterpenoids isolated from *H. angustifolia* exhibited remarkable cytotoxic activities against human colorectal cancer cells COLO 205 and gastric cancer cells AGS *in vitro*. In addition, Li et al. (2015) reported that the continuous treatment with the aqueous extract of *H. angustifolia* resulted in a significant reduction of tumor progression in HT1080 tumor bearing BALB/c nu mice. Further, a triterpenoid methyl helicterate (MH) isolated from *H. angustifolia* significantly decreased the levels of HBV DNA and cccDNA in the HBV-transfected cell line HepG2.2.15, which may contribute to the anti-HBV effect of *H. angustifolia* (Huang et al., 2013). Further, Li et al. (2015) investigated the free radicals (DPPH, ABTS, and OH · radicals) scavenging activities of aqueous and ethanol extracts of *H. angustifolia*. The study stated that the extracts displayed high activities in the assays tested. Most recently, the potential anti-diabetic effect of aqueous extract was identified by Hu et al. (2016), the result state that aqueous root extract from *H. angustifolia* efficiently enhanced glucose consumption in C2C12 myotubes and suppressed the increase of blood glucose levels in diabetic rats.

1.3. Target and structure of the thesis

H. angustifolia has received considerable attention as functional biomaterial for pharmaceutical and functional foods applications owing to its various biological activities. Previous works mainly focused on the isolation, determination and bioactivities identification of quinones, triterpenoids, lignins, and alkaloids from this plant. Up to the present, however, limit information is available on the bioactivity identification of its polysaccharides. An evidence from our previous study (Li et al., 2016) demonstrated that the polysaccharide rich fraction was found to exhibit significant antioxidant activity and play a major role in the immunomodulatory activity of this plant. Thus, proper isolation of native bioactive polysaccharides from *H. angustifolia*, evaluate the antioxidant and immunomodulatory activity both *in vitro* and *in vivo*, and determination of their structural features are the main targets of this study.

To achieve these objectives, the thesis was divided into five chapters.

Chapter 1 Introduction

In this chapter, the background of this research was introduced, including the introduction of polysaccharide, the structure, antioxidant and immunomodulatory activities of polysaccharides. In addition, state the phytochemical composition as well as the

pharmacological activity of *H. angustifolia*.

Chapter 2 Immunomodulatory activity of polysaccharides from *H. angustifolia* against breast cancer

In this chapter, a 4T1 breast tumor model in BALB/c mice was used to evaluate the *in vivo* immunomodulatory activity of HACP. Mice were orally administered with 100, 200, and 300 mg/kg of HACP for 15 days. At the end of the experiment, the tumor size changes, immune organ indices, CD4⁺/CD8⁺ ratios in spleen lymphocytes, and the immunomodulatory cytokines productions in the serum of tumor-bearing mice were determined.

Chapter 3 Purification and characterization of polysaccharide fractions from HACP

In this chapter, HACP was separated and purified into three fractions by using DEAE Sepharose Fast Flow and Sephacryl S-400 chromatography. The surface structure, monosaccharide composition and molecular weight of obtained fractions were identified.

Chapter 4 *In vitro* antioxidant and immunomodulatory effects of polysaccharide fractions

In this chapter, the *in vitro* antioxidant and macrophage cell activation ability of fractions SPF1-1, SPF2-1, and SPF3-1 were investigated. In addition, the relationships between polysaccharide structure and bioactivities are analysed as well.

Chapter 5 Conclusions and future researches

In this chapter, the main results were summarized, and the expected utilization of polysaccharides from *H. angustifolia* is put forward. In particular, the future study research of the polysaccharides was directed.

Table 1- 1 Polysaccharide drugs and healthy products of commercially available

Resource	Polysaccharide	Listed drugs
Plant	Ginseng polysaccharide	Ginseng Polysaccharide Injectionnn
	Astragalus polysaccharide	Astragalus polysaccharide injection
Microbal	Lentinan	Lentinan Injection; Lentinan capsules; Lentinus Edodes; Mycelia Polysaccharide Tablets
	Poria polysaccharide	Poria polysaccharide oral solution
	Ganoderma lucidum polysaccharide	Ganoderma lucidum polysaccharide capsules
	Dextran	Dextran 40 Glucose injection; Dextran 70 eye drops; Low molecule dextran
Animal	Chondroitin sulfate	Chondroitin Sulfate Tablets; Chondroitin sulfate (Chondroitin sulfate A sodium) capsules; Chondroitin sulfate (Chondroitin sulfate A sodium) injection
	Hyaluronic acid	Sodium hyaluronate injection; Sodium Hyaluronate Eye Drops

(Yu, Y., Shen, M., Song, Q., & Xie, J., 2018).

Table 1-2 Phytochemical composition of *H. angustifolia*

	Compound name	References
Triterpenoids	3 β - <i>O</i> - (trans-coumaroyl)betulinic acid 3 β - <i>O</i> -(trans-feruloyl)betulinic acid 3 β - <i>O</i> -(trans-coumaroyl)betulin 3 β - <i>O</i> -(cis-coumaroyl)betulin 3 β - <i>O</i> -(trans-caffeoyl)betulin 3 β - <i>O</i> -(trans-feruloyl)betulin methyl helicterilate methyl helicterate helicterilic acid cylicodiscic acid oleanolic acid pyracrenic acid cucurbitacin D cucurbitacin J	Chang, Ku et al. 2001
Naphthoquinone	heliquinone	Wang and Liu 1987
Mansonone	mansonone E mansonone F mansonone H	Chen et al. 1990
Steroids	β -sitosterol	
Alkaloid	heligenin A heligenin B helicterone A	Wang, Li et al. 2012
Flavonoid	potengriffioside A	Chen, Tang et al. 2006
Lignin	(7S,8R)-urolignoside (7S,8R)-dihydrodehydrodiconiferyl alcohol	
Phenolic compounds	rosmarinic acid protocatechuic aldehyde	



Figure 1-1 *H. angustifolia* used in this study

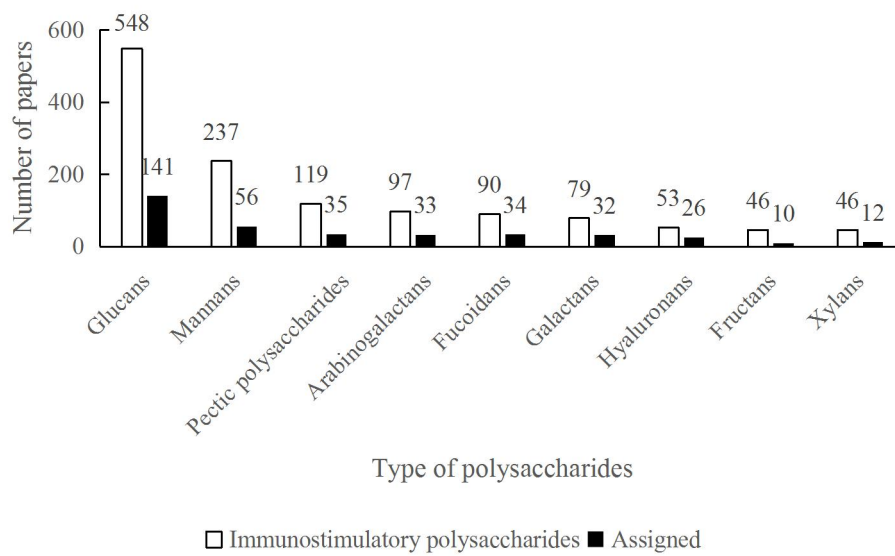


Figure 1-2 Number of papers with the topics “polysaccharides and immunostimulatory”
 These searches cover papers from 1936 until 2014.

(Ferreira, S. S. et al., 2015)

Chapter 2 Immunomodulatory activity of polysaccharides from *H. angustifolia* against breast cancer

2.1. Introduction

Every year, more than 2 million women are diagnosed with breast cancer worldwide, making it the second-leading cause of cancer-related death and the most common cancer among women worldwide. It is reported that about one in five women would die from this disease (Ginsburg et al., 2017; Gupta et al., 2012). The mortality of breast cancer usually results from the tumor metastatic spread to other organs, and the most common sites are the bone, followed by the lung and liver. Chemotherapy is one of the most commonly applied therapeutic modalities for breast cancer treatment. However, the chemotherapeutic agents used in the treatment are usually toxic to normal cells (Sun et al., 2014). Currently, accumulating evidence strongly suggests that the immune system plays a decisive role in controlling cancer development and progression (Ren et al., 2012; Wang et al., 2017), making the discovery of novel compounds with specific immunomodulatory activity and less toxicity of current interest to cancer researchers.

H. angustifolia has long been used as remedy to treat various diseases related to immune response. Its phytochemistry and pharmacological properties including antioxidation, antidiabetic, antiviral and anticancer activities have been already mentioned in chapter 1. Additionally, the polysaccharide-rich fraction from the aqueous extract of *H. angustifolia* has been found to have immunomodulatory activity *in vitro* in our very recent study (Li et al., 2016). Up to the present, however, whether the polysaccharide from *H. angustifolia* can regulate the immune system *in vivo* has not been disclosed yet.

2.2. Materials and methods

2.2.1. Plant material and chemicals

RPMI-1640 medium and fetal-calf serum was obtained from Gibco Life Technologies (Grand Island, NY, USA). FITC-anti-mouse-CD4 and PE-anti-mouse-CD8 antibodies, and Mouse TNF- α , IL-1 β , IFN- γ and IL-6 ELISA Kits were purchased from eBioscience (San Diego, CA, USA). CD34 primary antibody was from BD Pharmingen (San Jose, CA). The assay kits for superoxide dismutase (SOD) and CCK-8 were from Dojindo Molecular Technologies (Japan), and the CAT activity kit KO33-H1 was obtained from Arbor Assays (USA). Thiobarbituric acid reactive substance (TBARS) kit FR40 was purchased from Oxford Biomedical Research (USA). Red blood cell lysis buffer was purchased from

Sigma Aldrich, Inc. (Saint Louis, MO, USA). All the reagents used in this study were of analytical grade.

2.2.2. Polysaccharide extraction

The dry root powder of *H. angustifolia* (100 g) was defatted as described earlier (Wang et al., 2016). The defatted residue was then extracted with distilled water at 100°C for 3 h at a ratio of 1:10 (w/v). After 3 repetitions, the supernatant was collected, filtered, concentrated and mixed with 4 times of ethanol overnight at 4°C. This step was repeated three times to thoroughly remove the soluble ethanol. The resultant precipitate was deproteinized using the Sevag method, and the final solution was lyophilized to obtain the *H. angustifolia* crude polysaccharide (HACP).

2.2.3. Determination of chemical composition

The total phenolic content was determined using Folin-Ciocalteu reagent with Gallic acid as the standard. 0.1 mL of HACP were mixed with 0.4 mL of distilled water, and Folin–Ciocalteu reagent (1 mL) was added. After 3 min incubation, added 0.3 mL Na₂CO₃ (20%), the mixture was kept in the dark for 90 min. At last, the OD of the mixture was read at 725 nm using a UV- spectrophotometer. The total polyphenol content was expressed in milligrams of Gallic acid equivalents (GAE) per gram of the sample.

The total polysaccharide content of HACP was detected by using the phenol-sulfuric acid method (DuBois et al., 1956). The uronic acid content of SPF3-1 was determined by modified carbazole method according to a previous research (Bitter & Muir, 1962). And the protein content was determined with the protein quantification kit according to the manufacture procedure.

2.2.4. Cell culture

Mouse mammary tumor cell line 4T1 was purchased from Riken Cell Bank (Tsukuba, Japan). Cells were cultured in RPMI-1640 media supplemented with 10% FBS, penicillin (100 U/mL) and streptomycin (100 µg/mL) at 37°C in a 5% CO₂ incubator.

2.2.5. Cytotoxicity effect on 4T1 cells

To determine the cytotoxicity of HACP on 4T1 cells, the MTT assay was employed as described previously (Li et al., 2016). After 4T1 cells (1×10^5 cell/well) were seeded into a 96-well plate, the cells were incubated with various concentrations of HACP for 48 h (12.5-400 µg/mL). The cell viability was determined at 450 nm using a Model 550 microplate reader (BIO-RED, Tokyo, Japan).

2.2.6. Sub-acute toxicity study

Five-week-old female BALB/c mice were purchased from Beijing HFK Bioscience Co., Ltd. (Beijing, China). The mice were maintained under controlled conditions with a constant temperature of $23 \pm 1^\circ\text{C}$, humidity of $55 \pm 5\%$ and a 12 h light/dark cycle. The mice were acclimatized for 1 week before being used for the experiment.

Female BALB/c mice (6 weeks old), weighing 17 ± 0.5 g, were orally administered with 1000 mg/kg of HACP (0.2 mL, every day) for 15 days. During the treatment period, mice were observed daily for any sign of toxicity, and their body weights were examined once every three days.

2.2.7. Design for mouse experiment

In total, thirty mice of 6 weeks of age were used in this experiment. 4T1 cells (5×10^5 cells resuspended in 200 μL PBS) were subcutaneously (s.c.) inoculated at the mammary fat pad of the mice (24 mice were used in total), and the remaining 6 mice were recognized as Group 1, namely, the normal control group. Six days after tumor cell inoculation, the tumor-injected mice were randomly divided into four other groups ($n = 6$): (1) Group 2: tumor control group; (2) Group 3: 100 mg/kg of HACP; (3) Group 4: 200 mg/kg of HACP; and (5) Group 5: 300 mg/kg of HACP. That is, HACP was administered orally to each group at different dosages (100, 200, and 300 mg/kg) in the three HACP treated groups, respectively. The tumor control (Group 2) and normal control groups (Group 1) were treated with distilled water. All the treatments lasted for 15 days. The body weight and tumor volume of each mouse were measured once every three days. The volume of the tumor was calculated using the following formula: $V (\text{mm}^3) = (a \times b^2) / 2$ (Collins & Yuan et al., 2003), where a and b represent the maximum and minimum diameter (mm), respectively. On day 21, the blood of each animal was collected from the eyeball for further analysis. Meanwhile, organs, such as the tumor, lung, spleen and thymus, were removed from each mouse, weighed, and sampled for further use. Spleen and thymus indices were calculated according to the following equation: organ index = weight of organ (mg) / body weight (g) (Huang et al., 2016).

2.2.8. Histopathology staining

Tumor tissues and lungs were fixed in 10% formalin. The tissues were then cut into 3-mm-thick sections and subjected to histology analysis with hematoxylin and eosin (H&E) staining. To detect the microvessel density in the tumors, slides were also processed for CD34 staining as described previously (Pan et al., 2015). Tumor burden in the lungs was measured using ImageJ (NIH, USA) as described by Luo et al. (2014).

2.2.9. Determination of spleen lymphocyte phenotype

The spleen lymphocytes were isolated as described previously (Zhang et al., 2017) with some modifications. The spleens from each mouse were collected under aseptic conditions. After washing with cold PBS 2 times, the spleens were scraped by glass pieces in a cell culture plate containing 2 mL of PBS. The cells were then passed through a 200- μ m cell mesh to obtain a single cell suspension. After centrifugation, red blood cell lysis buffer was used to remove erythrocytes, and the splenic lymphocytes were washed and re-suspended in RPMI 1640 medium. Cell viability (over 90%) was assessed microscopically by trypan blue dye. The single splenocyte suspensions were adjusted to 1×10^6 cells/mL, and immunostained with 0.25 μ g FITC-CD4⁺ and PE-CD8⁺ antibodies under dark conditions for 30 min. After incubation, the lymphocytes were rinsed three times with 2 mL of PBS and centrifuged at 1500 rpm for 5 min. Thereafter, the CD4⁺ and CD8⁺-cell populations were analyzed with a FACScan flow cytometer (Becton Dickinson, San Jose, CA).

2.2.10. Antioxidant enzyme activities and cytokines production in mice serum

The blood samples of each mouse were centrifuged for 20 minutes at 3000 rpm and 4°C to obtain the serum. The TNF- α , IL-1 β , IFN- γ , and IL-6 productions in the serum were identified using commercial ELISA kits according to the manufacturer's instructions. And the antioxidant enzymes of Catalase (CAT), superoxide dismutase (SOD), and malondialdehyde (MDA) levels in the mice serum were measured by colorimetric assay kits according to the manufacturer's instructions.

2.2.11. Splenocytes proliferation and natural killer (NK) cell activity

The splenocytes proliferation was determined according to a previous study (Huang et al., 2016). 100 μ L of splenocytes from each mice group were seeded into a 96-well plate (5×10^6 cell/well) and cultured for 48 h at 37°C in a 5% CO₂ incubator. The cell viability was identified by a CCK-8 assay.

The NK cell activity was identified according to previous literature (Tu et al., 2008). Briefly, the target cells (4T1 cells, 2×10^4 cells/well) were seeded in a 96-well plate. Then, splenocytes from each animal group were added into each well (1×10^6 cells/well) and used as effector cells. After incubation for 24 h, the cell viability was identified using a CCK-8 assay (Li et al., 2017). The NK cell activity was calculated using the following equation: NK cell activity (%) = $100 \times (OD_T - (OD_S - OD_E)) / OD_T$, where OD_T means the optical density of the target control cells, OD_S is the optical density of the tested sample,

and OD_E is the optical density of the effector cell control.

2.2.12. Statistical analysis

All the data were expressed as the mean \pm standard deviation (SD), and the results were taken from at least three independent experiments performed in triplicate. In addition, the data were analyzed using one-way analysis of variance (ANOVA) with Duncan's multiple-range test. $p < 0.05$ was considered statistically significant.

2.3. Results and discussion

2.3.1. Chemical composition of HACP

In this Chapter, the crud polysaccharide HACP was extracted from *H. angustifolia* with a yield of 4.04%. Chemical composition analysis indicated that HACP contains 50.32% polysaccharide, 5.62% protein, and 9.66% total phenolic compounds.

2.3.2. Non-toxicity of HACP on 4T1 cells *in vitro*

According to Fig. 2-1, after culture with HACP at 12.5-400 $\mu\text{g/mL}$ for 48 h, all the 4T1 cell survival rates were greater than 90%. According to U.S. National Cancer Institute (NCI), plant extract with an IC₅₀ value less than 20 $\mu\text{g/mL}$ is considered to be cytotoxic (Vijayarathna & Sasidharan, 2012). Thus, HACP could be regarded as non-cytotoxic.

2.3.3. HACP does not show any acute toxicity *in vivo*

Before the *in vivo* anti-tumor assay was carried out, a daily oral toxicity study was conducted using 1000 mg/kg of HACP treatment for 15 days. During this period, the mice did not show any abnormal behavior or side effects associated with toxicity. Thus, three treatment doses, 100 mg/kg, 200 mg/kg, and 300 mg/kg of HACP were selected for determination of the inhibition effect on 4T1 tumor growth.

2.3.4. HACP inhibited tumor growth in 4T1 cell-bearing mice

As shown in Fig. 2-2A, at the beginning of the experiment, the tumor volume remained almost the same in each group. From day 12 on, a rapid development of tumor size in the control group was noticed, and the maximum tumor volume ($791.4 \pm 76.0 \text{ mm}^3$) was detected in the mice of the tumor control group at the end of experiment. In contrast, almost $48.07 \pm 5.71\%$, $55.31 \pm 4.18\%$ and $62.97 \pm 5.42\%$ of inhibition in tumor progression were recorded for the 100 mg/kg, 200 mg/kg, and 300 mg/kg of HACP treated groups, respectively. The HACP application not only decreased the tumor volume but also reduced the tumor weight obviously (Fig. 2-2B). As shown, 100 mg/kg, 200 mg/kg and 300 mg/kg of HACP treatment inhibited the tumor weight by $34.58 \pm 10.20\%$, $57.80 \pm 8.65\%$, and $67.71 \pm 5.80\%$, respectively. No significant change in the mice body weight

was observed during the treatment period (Fig. 2-2D), indicating the nontoxic effect of HACP during the 15-day oral administration.

2.3.5. HACP inhibited 4T1 mammary metastasis to lung

Due to the high metastatic ability, 4T1 tumor can easily transfer to the lung, liver, and bone (Tao et al., 2008). Fig. 2-3 shows the representative histological sections of lungs from the control and 300 mg/kg HACP treated groups. As indicated by the arrows, the tumor area in the lungs of the tumor control group were approximately 13.74%. By contrast, 300 mg/kg of HACP treatment was found to decrease the tumor area to 2.45% of the total lung area. This result suggests that HACP is effective in decreasing tumor metastasis to the lung.

2.3.6. HACP induced apoptosis and angiogenesis reduction in tumors

The architecture and morphology of the tumor cells were analyzed by H&E staining. As shown in Fig. 2-4, the control group showed the normal cellular morphology of 4T1 cell line. However, the HACP treated groups reflected the characteristic features of apoptosis, cell shrinkage and nuclear chromatin condensation. The angiogenesis expression of tumor tissues was analyzed by CD34 immunohistochemistry staining. The staining intensity of CD34 was significantly reduced in the HACP treated groups. These observations are consistent with the reduced tumor size and weight in the HACP treatment groups in comparison to the tumor control group.

2.3.7. HACP increased the immune organ indices, as well as CD4⁺/CD8⁺ ratios in spleen lymphocyte

As shown in Table 2-1, after consecutive administration for 15 days, the spleen and thymus indices in the HACP treated mice increased obviously compared with the mice in the tumor control group, indicating an elevated immune response in the HACP treated 4T1 tumor-bearing mice. As is well known, CD4⁺ and CD8⁺ are T helper (Th) and T cytotoxic (Tc) lymphocytes, respectively. A high ratio of CD4⁺/CD8⁺ in favor of tumor suppression has been proven by a previous study (Shen et al., 2013). The results from flow cytometric analysis demonstrated that the ratio of CD4⁺/CD8⁺ in the spleen of tumor control mice was significant lower ($p < 0.05$) than those in the HACP treated groups, in support of the fact that HACP possesses the tumor suppression effect on 4T1 tumor-bearing mice, which is probably attributed to the lymphocyte activation strategies.

2.3.8. HACP regulated the antioxidant enzymes and cytokines production in serum of tumor-bearing mice

In this work, the cytokine levels of TNF- α , IL-6, IFN- γ and IL-1 β in the mice serum were identified. Fig. 2-5A shows that treatment with HACP enhanced TNF- α production in a dose-dependent manner with the highest level (452.7 ± 85.79 pg/mL) achieved at 300 mg/kg group, which was significantly higher than the tumor control group (102.86 ± 48.46 pg/mL). A similar result was also obtained in IL-1 β and IFN- γ generation. As shown in Figs. 2-5B and 2-5C, 300 mg/kg of HACP treatment increased the production of IL-1 β and IFN- γ by 4.86 and 1.55-fold compared to the tumor control group. In contrast, IL-6 production was noticed to decrease from 235.71 ± 25.74 pg/mL to 91.88 ± 5.17 pg/mL after 300 mg/kg HACP treatment (Fig. 2-5D). These findings suggest that HACP treatment exhibited immunomodulatory effects on 4T1 tumor-bearing mice by up-regulating the TNF- α , IFN- γ , and IL-1 β levels and down-regulating the IL-6 production.

The serum levels of CAT, SOD and MDA were also measured in the present study. The results from Fig. 2-6 show that HACP treatment obviously reduced MDA generation in the mice serum compared with the tumor control group. In particular, the 300 mg/kg HACP treatment maintained similar MDA level as the basal condition. In addition, HACP administration improved the activities of CAT and SOD in the serum of 4T1 tumor-bearing mice compared with the control group ($p < 0.05$); however, a dose-dependent effect was not observed.

2.3.9. Effect of HACP on splenocytes proliferation and NK cell activity

NK cell activity assays are usually used to reflect the body's *in vitro* cellular immune response (Zhang et al., 2005). In this study, HACP was found to significantly enhance the killing activity of NK cells in the 4T1 tumor-bearing mice (Fig. 2-7). For the 300 mg/kg HACP treated group, an NK cell activity of $50.17 \pm 5.28\%$ was achieved, which is significantly higher than the tumor control group ($25.12 \pm 4.72\%$).

The stimulatory effect of HACP on mouse splenocyte proliferation is shown in Fig. 2-8. Compared to the normal and tumor control groups, HACP treatment at 200 mg/kg or 300 mg/kg significantly promoted splenocyte proliferation. This observation implies that the increases mouse spleen growth by HACP is probably attributed to the stimulation effect on splenocyte proliferation.

2.4. Discussion

In the present study, the *in vivo* immunomodulatory effect of HACP was first investigated using a 4T1 tumor-bearing BALB/c mouse model. The results suggested that after 15 days' administration, HACP was demonstrated to be effective in decreasing the

tumor growth and lung metastasis. Since HACP did not show any cytotoxic effect on 4T1 cells *in vitro* (Fig. 2-1), it could be concluded that the *in vivo* tumor suppression effect was not brought about by its cytotoxic effect. According to previous works (Cho & Leung 2007; Schepetkin & Quinn 2006; Wang et al., 2015), many polysaccharides extract from traditional plants possess anticancer activities in an indirect manner by regulating the host immune response. For this reason, we further investigated the effects of HACP on immunity in 4T1 tumor-bearing mice to analyze the underlying antitumor mechanisms.

As the most important immune organs, the spleen and thymus directly participate in tumor suppression and antitumor cytokine generation (Wang et al., 2015; Zhang et al., 2004). Generally, a higher organ index indicates a stronger immune capability (Huang et al., 2016; Zhu et al., 2016). According to Table 2-1, with a spleen index of 28.96 ± 0.45 mg/g in the 300 mg/kg HACP treatment group (TC group, 15.09 ± 1.60 mg/g), HACP was found to significantly elevate spleen organ growth, which may result from its potent splenocytes proliferation ability (Fig. 2-8). The spleen indices for the 4T1 tumor-bearing mice were significantly ($p < 0.05$) higher compared to the normal group, which is in agreement with previous reports that, to some extent, found the spleen weights of mice with breast cancer to be much higher than those in normal mice (Aragon et al., 2014; Razali et al., 2016). The CD8⁺ T cell can specifically and directly kill cancer cells, thus exhibiting cytotoxic effects. On the other hand, CD4⁺ cells, namely, helper T cells, always help activate other immune cells, including macrophages and NK cells, by releasing cytokines (Zhu et al., 2016). The present results suggest that HACP could significantly ($p < 0.05$) increase the percentage of CD4⁺ and CD8⁺ T cells, and up-regulate the ratio of CD4⁺/CD8⁺ cells, indicating their participation in antitumor activity *in vivo*.

Since cytokines play a vital role in the regulation of the host immune response, the identification of cytokine levels is often used as a parameter to evaluate the immunomodulatory effect (Razali et al., 2016). Numerous studies have demonstrated that TNF- α plays a pivotal role in the regulation of immunoregulatory mediator expression and antitumor activity (Baugh & Bucala 2001; Zhang et al., 2017). In the present study, after 15 days' treatment, an almost 4-fold increase in TNF- α production was detected in the 300 mg/kg HACP treatment group compared with the tumor control group. IFN- γ and IL-1 β have many functions and are very important in the host defense against the tumor (Razali et al., 2016; Zhang et al., 2013). The application of HACP was found to efficiently stimulate mouse serum IFN- γ and IL-1 β release in this study, suggesting that HACP could

activate the immune response of 4T1 tumor-bearing mice through the up-regulation of TNF- α , IFN- γ and IL-1 β . Moreover, IL-6, as a pro-angiogenic factor, is essential for breast tumor growth and metastasis (Aragon et al., 2014). In the present study, the tumor control group with the highest tumor size and lung metastasis status demonstrated a significant increase in the IL-6 production, while the HACP treated mice were found to maintain similar IL-6 levels as their normal conditions (Fig. 2-5). This result is consistent with Zhang et al. (2017), who also observed a reduced release of IL-6 after administration of Royal Jelly for 42 days using a 4T1-tumor bearing mice model. It is believed that the lower level of IL-6 induced by HACP contributes to the suppression of tumor progression.

It is well known that excessive oxidative stress is an underlying cause of cancer (Telo et al., 2017). Antioxidant enzymes are essential in protecting the host against oxidative stress (Huang et al., 2016; Zeng et al., 2017), among which CAT is a very important enzyme that can detoxify hydrogen peroxide into water, and SOD plays a major role in host defense against oxygen toxicity (Murk et al., 2002). Moreover, MDA is one of the most important end-products of lipid peroxidation, and its level in the serum signals the degree of lipid peroxidation. In the present study, HACP administration significantly improved the activities of CAT and SOD, and decreased MDA levels in the serum of 4T1 tumor-bearing mice (Fig. 2-6), suggesting that HACP exhibits antioxidant effects, which may partially contribute to its antitumor effects.

2.5. Summary

All the above findings suggest that HACP could enhance the immune response in 4T1 tumor-bearing mice. The small size and reduced vascularization in the tumors and decreased lung metastasis in the mice clearly reflect the beneficial effects of the immune response regulated by HACP treatment. Thus, HACP could be developed as a new product for breast cancer treatment with immunomodulatory activity in the future.

Table 2- 1 Effects of HACP on immune organ indices, and T cell subsets in the spleen of tumor bearing mice.

Group	Spleen indices (mg/g)	Thymus indices (mg/g)	CD4⁺ (%)	CD8⁺ (%)	CD4⁺/CD8⁺
NC	7.54 ± 2.72 ^d	1.68 ± 0.29 ^c	11.33 ± 1.48 ^c	4.70 ± 1.21 ^a	2.46 ± 0.14 ^a
TC	15.09 ± 1.60 ^c	1.69 ± 0.27 ^c	8.59 ± 0.92 ^c	4.18 ± 0.22 ^b	2.05 ± 0.18 ^b
100 mg/kg	20.66 ± 3.32 ^b	2.42 ± 0.33 ^b	13.59 ± 3.62 ^b	6.44 ± 1.56 ^a	2.10 ± 0.12 ^b
200 mg/kg	19.11 ± 4.70 ^b	2.59 ± 0.19 ^b	12.48 ± 1.16 ^b	5.03 ± 0.46 ^a	2.48 ± 0.03 ^a
300 mg/kg	28.96 ± 0.45 ^a	2.97 ± 0.21 ^a	17.35 ± 3.04 ^a	6.72 ± 1.84 ^a	2.64 ± 0.31 ^a

Results are represented as the mean ± SD (n = 6). NC: normal control, TC: tumor control.

^{a-d}Values in the same column with different superscript letters indicate a significant difference ($p < 0.05$).

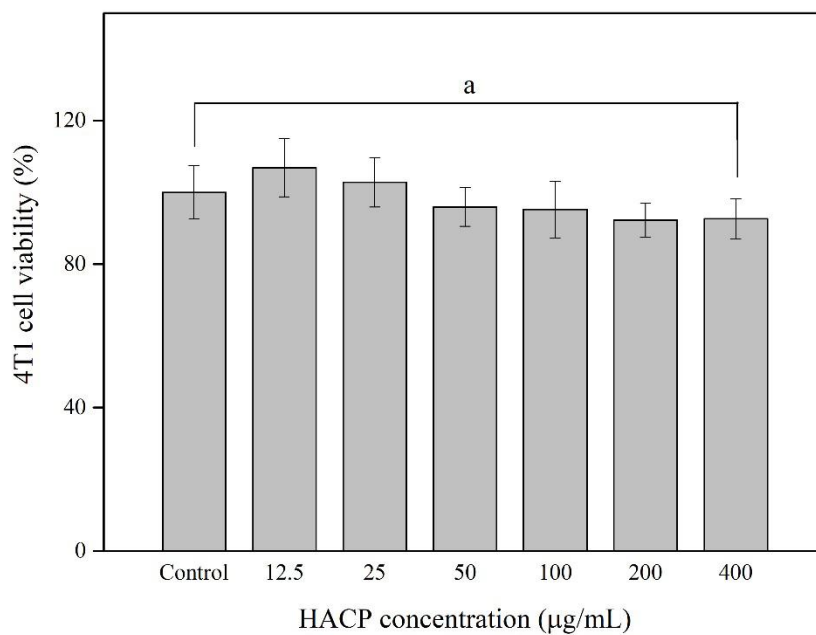


Figure 2-1 *In vitro* cytotoxic effect of HACP on 4T1 breast tumor cells

Cells were cultured with HACP (12.5-400 µg/mL) for 48 h. The results are represented as the mean \pm SD ($n = 6$). Bar values with the same letter (a) indicate no significant difference from the control group ($p > 0.071$, for all HACP treated groups).

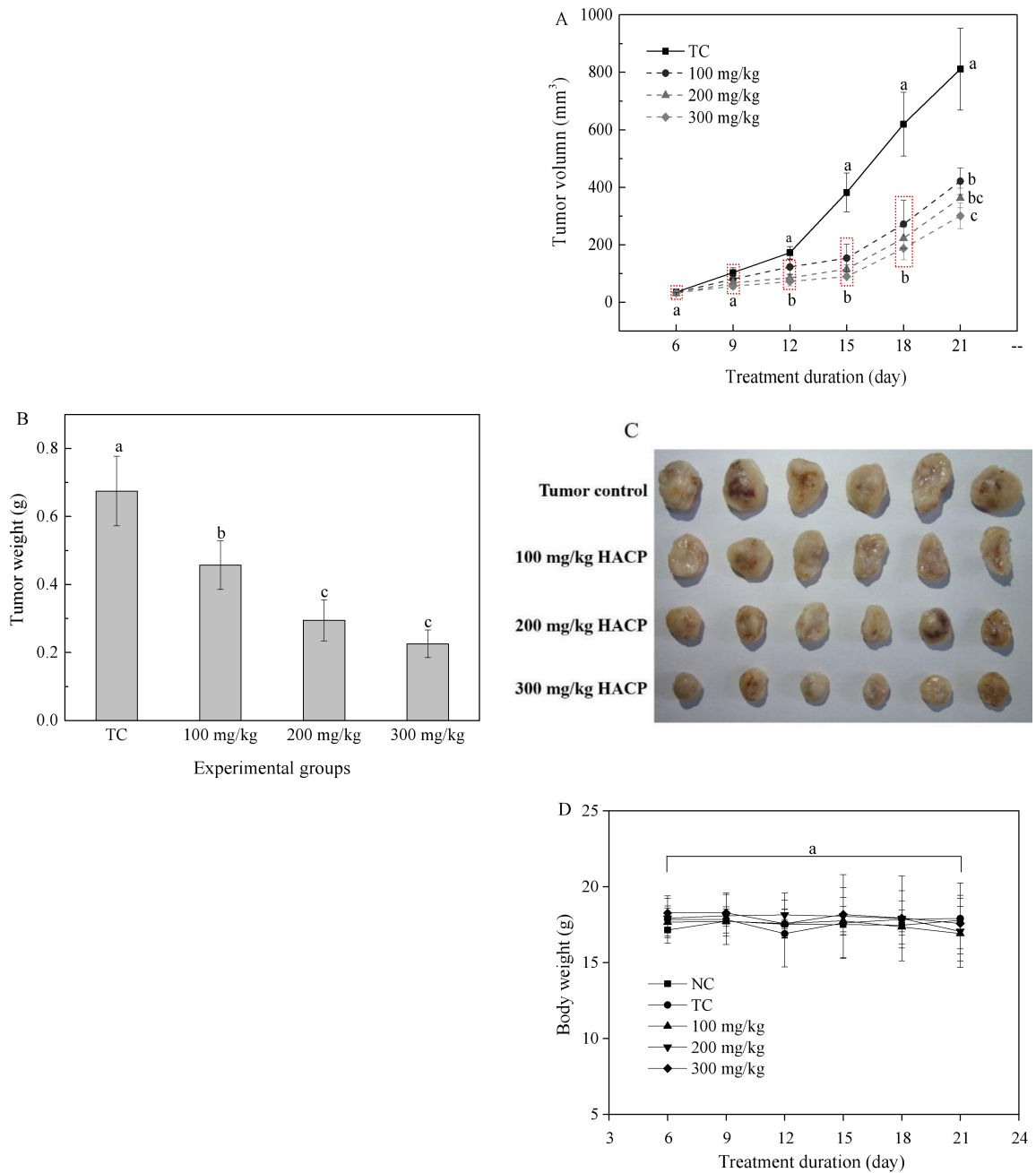


Figure 2-2 Inhibition effects of HACP on 4T1 tumor growth

(A) Tumor volumes in 4T1 tumor-bearing mice, (B) Tumor weight of 4T1 tumor-bearing mice, (C) Tumors sampled from experiment groups, and (D) Changes in body weight of the mice. The results are represented as the mean \pm SD ($n = 6$). NC: normal control, TC: tumor control. Bar values with different letters (a–c) indicate a significant difference ($p < 0.05$).

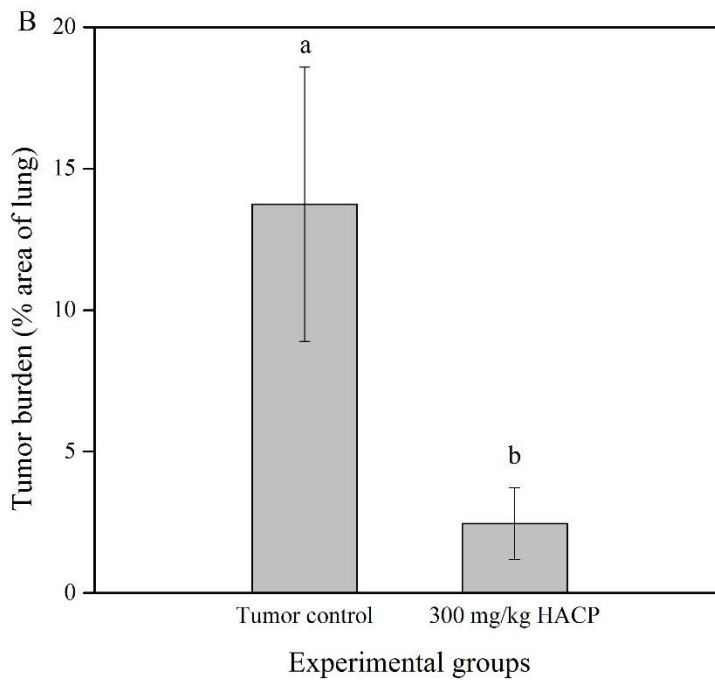
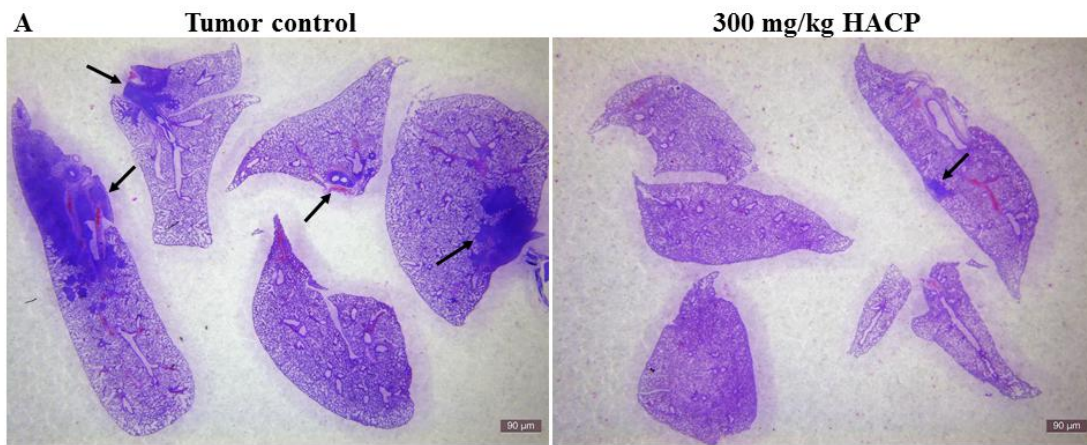


Figure 2-3 Inhibition effects of HACP on 4T1 tumor metastasis to lung

(A) H&E staining of lung organs of 4T1 tumor-bearing mice, (B) Tumor burden of the lungs in 4T1 tumor-bearing mice. The results are represented as the mean \pm SD ($n = 5$). Bar values with different letters (a, b) indicate a significant difference ($p < 0.05$).

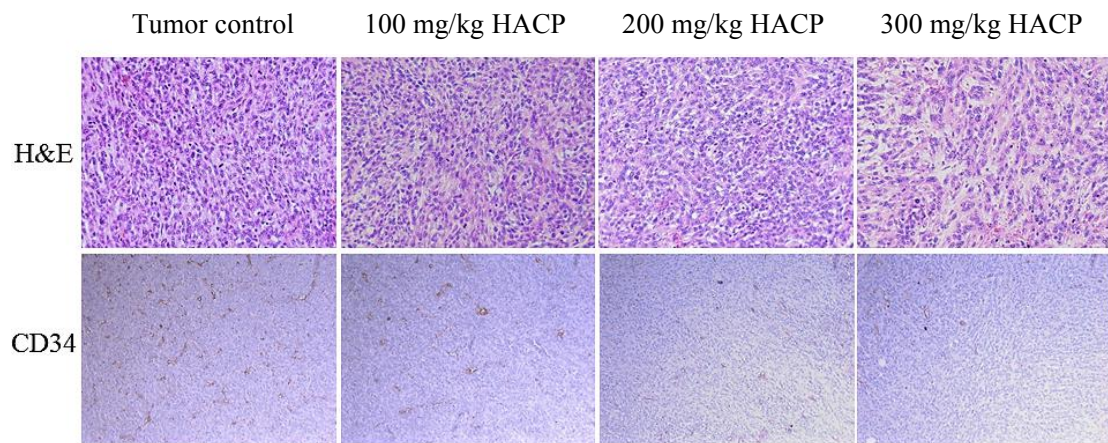


Figure 2-4 H&E staining and CD34 immunohistochemistry of tumor tissues from 4T1 tumor-bearing mice

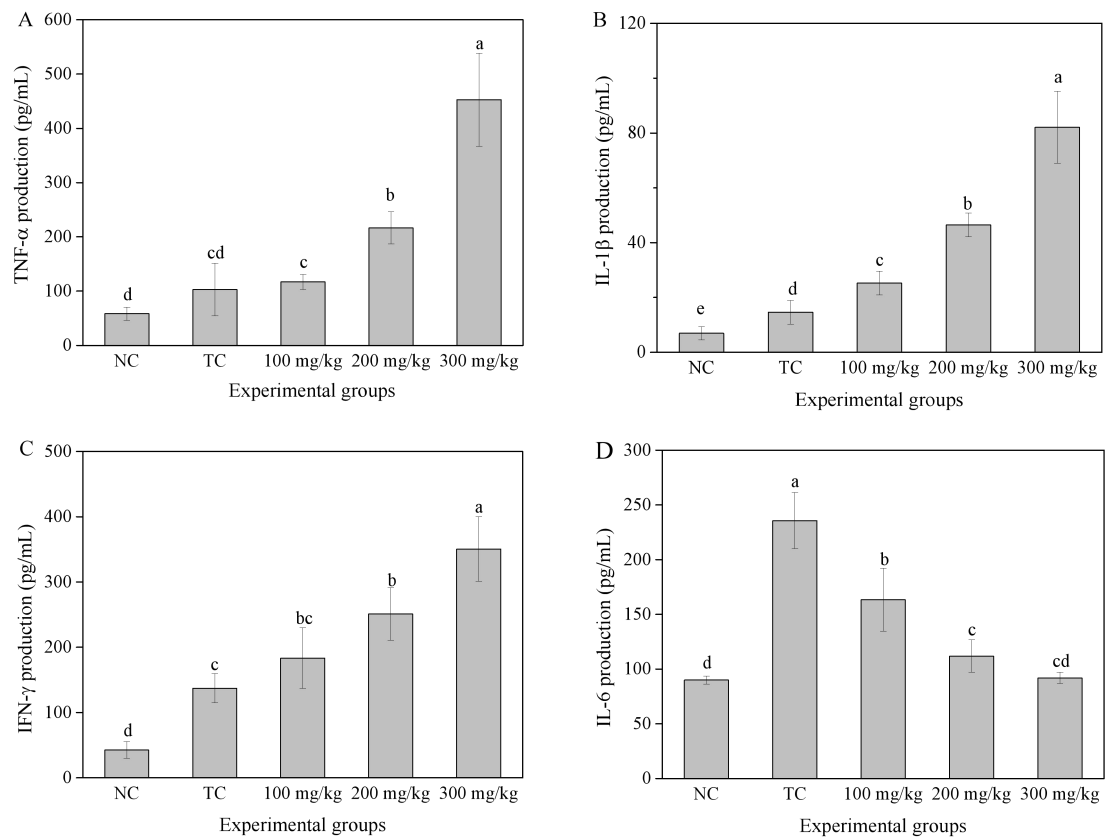


Figure 2-5 Cytokine production in mice serum

(A) TNF- α production, (B) IL-1 β production, (C) IFN- γ levels, and (D) IL-6 production in mouse serum. The results are represented as the mean \pm SD ($n = 6$). NC: normal control, TC: tumor control. Bar values with the different letters (a–e) indicate a significant difference ($p < 0.05$).

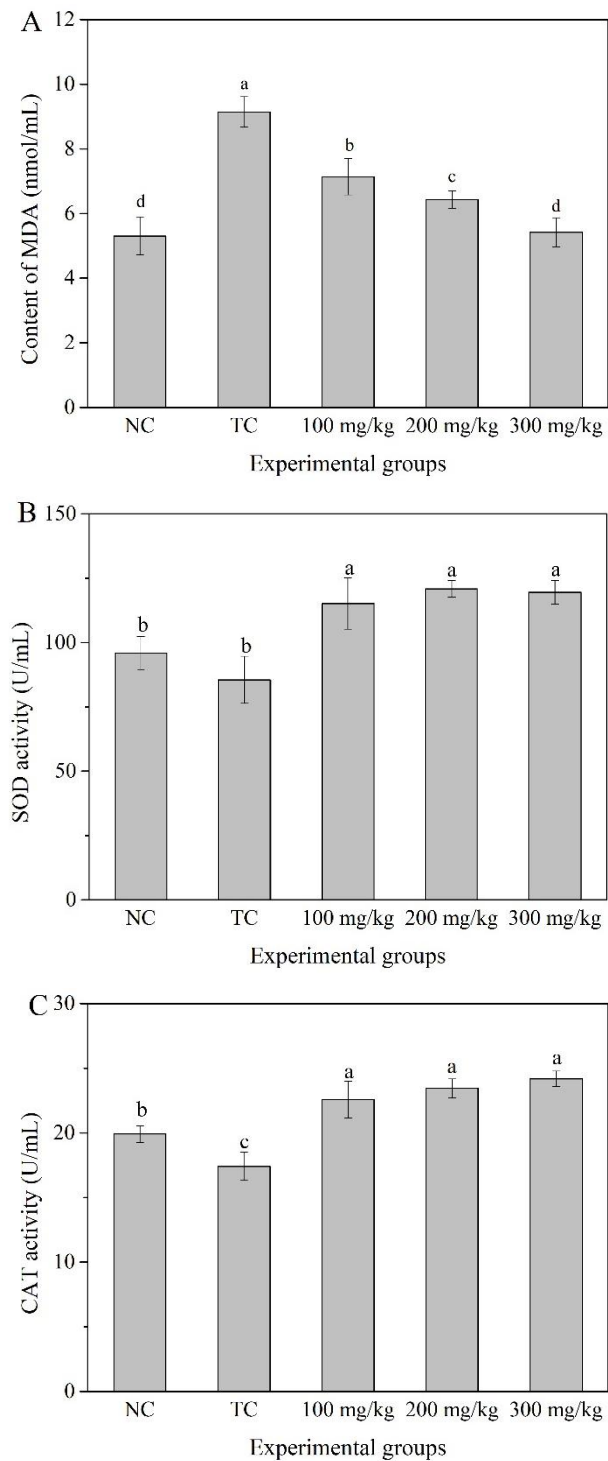


Figure 2-6 Antioxidant enzyme levels in the serum of 4T1 tumor-bearing mice

(A) MDA levels in mice serum, (B) SOD activity, and (C) CAT activity in the serum of 4T1 tumor-bearing mice. The results are represented as the mean \pm SD ($n = 6$). NC: normal control, TC: tumor control. Bar values with the different letters (a–d) indicate a significant difference ($p < 0.05$).

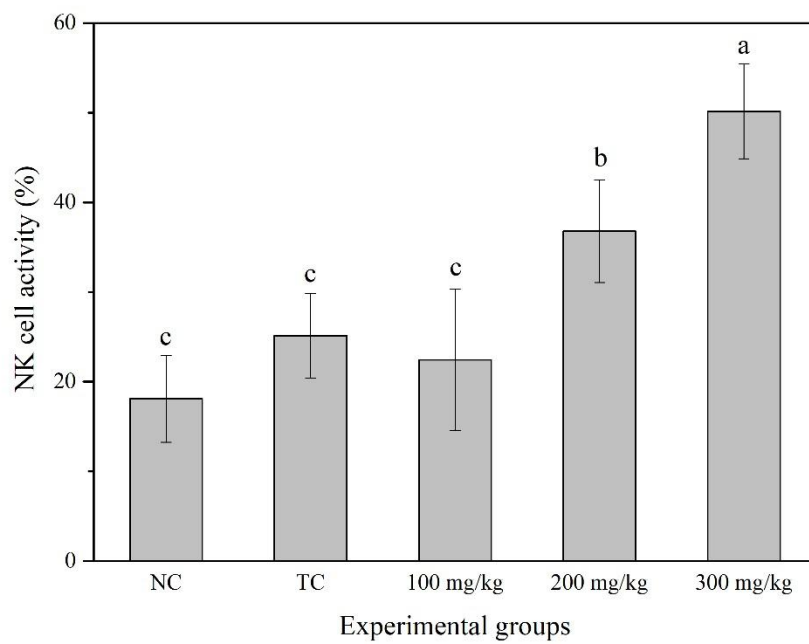


Figure 2-7 Effect of HACP on the NK cell activity of 4T1 tumor-bearing mice

The results are represented as the mean \pm SD ($n = 6$). NC: normal control, TC: tumor control. Bar values with different letters (a–c) indicate a significant difference ($p < 0.05$).

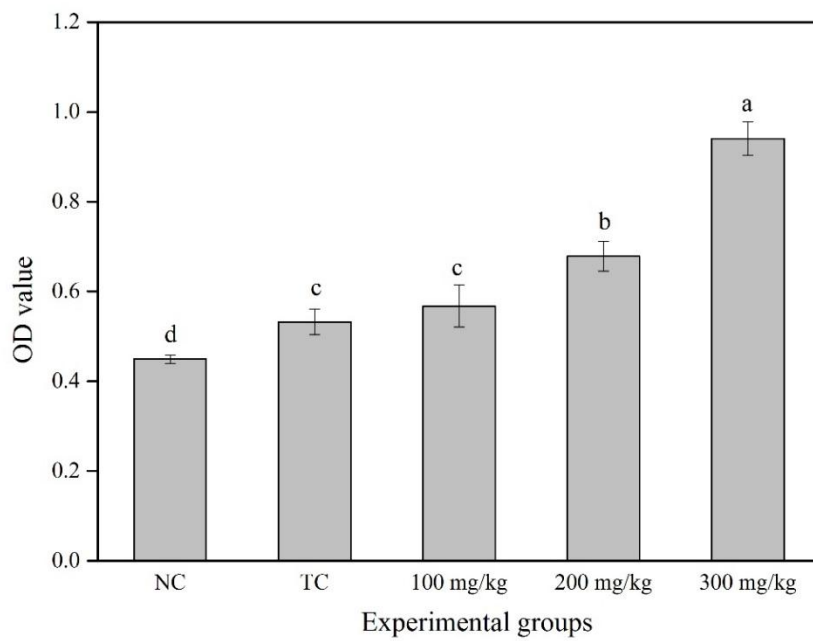


Figure 2-8 Effect of HACP on splenocytes proliferation of 4T1 tumor-bearing mice
The results are represented as the mean \pm SD ($n = 6$). NC: normal control, TC: tumor control. Bar values with the different letters (a–d) indicate a significant difference ($p < 0.05$).

Chapter 3 Purification and characterization of polysaccharide fractions from HACP

3.1. Introduction

Polysaccharide is a high molecular weight polymer, which consist of at least ten monosaccharide joined by glycosidic linkages (Wang et al., 2016). Because of the differences in monosaccharide compositions, glycosidic linkages, and degrees of polymerization, the structure of polysaccharide is far more complicated than protein and nucleic acid. Furthermore, other factors, such as extraction methods and purification procedures are evidenced to have significant influence on the physicochemical and structural properties of polysaccharides.

Generally, polysaccharides are present together with proteins, lipids, and lignin. However, the impure compounds may influence the biological activities of the polysaccharides, which may even cause undesirable toxicity (Yu et al., 2018). In other words, pure polysaccharides could enable the safe, bioactivities, and also enable the investigation of structure/activity relationship. Thus, further purification of bioactive polysaccharides from crude extracts, such as ethanol precipitation, ion-exchange chromatography, and gel filtration are of high importance. Among them, anion exchange column chromatography is the most commonly applied method in purification of polysaccharides at present (Shi, 2016). Polysaccharide solution can be concentrated and preliminarily purified through this method.

In this chapter, three major polysaccharide fractions of HACP was purified stepwise with DEAE Sepharose Fast Flow and Sephacry S-400 column chromatography, successfully. And the primary structure features and molecular weight of the obtained polysaccharide fractions were determined.

3.2. Materials and methods

3.2.1. Chemicals and reagents

DEAE Sepharose Fast Flow and Sephacry S-400 chromatography were obtained from GE Healthcare Bio-sciences (Uppsala, Sweden). Carbazole and D-Galacturonic acid were purchased from Wako (Japan). Protein Quantification Kit-Rapid was obtained from Dojindo Molecular Technologies (Japan). All the reagents used in this study were of analytical grade.

3.2.2. Purification of HACP

The HACP was purified sequentially by using DEAE Sepharose Fast Flow anion-exchange chromatography and Sephacryl S-400 size exclusion chromatography. Briefly, approximately 300 mg of HACP was dissolved in 10 mL of ultrapure water and applied to DEAE Sepharose Fast Flow column (450 × 40 mm), followed by eluting stepwise with ultrapure water, 0.1, 0.3, and 0.5 M NaCl at a flow rate of 3 mL/min. The elution (6 mL/tube) of each fraction was collected and detected by using the phenol-sulfuric acid method (DuBois, Gilles, Hamilton, Rebers, & Smith, 1956). Totally 600 mL of wash solution was used for each fraction. Then, the fractions were concentrated at 50 °C by rotary evaporation under reduced pressure, and lyophilized to obtain SPF1, SPF2, SPF3 and SPF4, respectively. Fraction SPF1, SPF2, SPF3 were further fractionated with Sephacry S-400 column (450 × 20 mm) eluted with ultrapure water at a flow rate of 0.5 mL/min. The fractions (3 mL/tube) were collected and analysed by the upper way. Finally, the major fraction named SPF1-1, SPF2-1, and SPF3-1 were then collected, and lyophilized to powder.

3.2.3. Chemical composition and molecular weight (Mw)

The uronic acid content of polysaccharide fractions were determined by modified carbazole method according to a previous research (Bitter & Muir, 1962). And the protein content was determined with the protein quantification kit according to the manufacture procedure.

The neutral monosaccharaides composition was determined by using high performance anion exchange chromatography (HPAEC) with pulsed amperometric detection (PAD). Fraction SPF1-1, SPF2-1, and SPF3-1 (10 mg) were hydrolysed with 4 M of trifluoroacetic acid (TFA, 4 mL) at 120 °C for 4 h in a sealed tube. After cooling to ambient temperature, the excess TFA was removed, and then the residue was re-dissolved in 10 mL of ultrapure water, the resultant solution was diluted for 50 times and filtered through a 0.22 µm filter. The derivatives were then performed on a Dionex HPAEC-PAD system (Dionex, USA) with an advanced gradient pump and eluent degas module. The monosaccharide composition was identified as described previously (Cai et al., 2016). The Mw was determined by using a high-performance size elusion chromatography instrument equipped with multi-angle laser light scattering and refractive index (HPSEC-MALLS-RID) system according to the method described by Yang et al. (2016) with some modifications. The HPSEC-MALLS-RID system consists of a pump (e2695, Waters, USA), a HPSEC columns (TSKgel SuperMultipore PW-M, TOSOH, Japan), a

MALLS detector (DAWN HELEOSII, Wyatt Technology, Santa Barbara, CA, USA), and a RI detector (OPTILAB T-rex, Wyatt Technology, Santa Barbara, CA, USA). 10 mg of polysaccharide fraction was dissolved in 1 mL of distilled water and filtered through a 0.22 μm filter. Twenty μL of solution was injected into the HPSEC column and eluted with distilled water at a flow rate of 0.5 mL/min.

3.2.4. FTIR and UV spectroscopy

The structure features of polysaccharides were analysed by using a Fourier transform infrared spectrophotometer (FT/IR-300, JASCO, Japan). Samples were ground with potassium bromide (KBr) powder and pressed into a pellet for FTIR measurement at a frequency range of 4000-500 cm^{-1} .

For UV spectrum analysis, the aqueous solution of SPF1-1, SPF2-1, and SPF3-1 at 1.0 mg/mL was scanned at the wavelength from 190 to 600 nm on a UV-vis spectrophotometer (UV-3100PC, SHIMADZU, Japan).

3.2.5. Nuclear magnetic resonance (NMR) analysis

Polysaccharide fractions (7 mg) were dissolved in 0.6 mL D_2O in an NMR tube. ^1H NMR analysis was performed on a Bruker AVANCE-600 NMR Spectrometer.

3.2.6. SEM analysis

SEM was used to characterize the micro-structures and surface morphologies of materials in the fractions. Dried samples of the three purified fractions were fixed on a specimen holder, coated using ion beam sputtering deposition, and then examined at a 5 KV acceleration voltage in a vacuum specimen chamber. The shape and surface characteristics were observed, and images were collected using a scanning electron microscope (JSM6330F, Japan), followed by magnification at 250-500 \times .

3.3. Results and discussion

3.3.1. Purification and separation of HACP

The HACP was separated with a DEAE Sepharose Fast Flow chromatography as shown in Fig. 3-1A. Result indicates that HACP was mainly composed of four fractions (SPF1, SPF2, SPF3, and SPF4) which were eluted with the ultrapure water, 0.1 M, 0.3 M, and 0.5 M NaCl, yielding about 15.3%, 12.7%, 22.3%, and 8.1% of the amount of HACP, respectively. The fractions SPF1, SPF2, and SPF3 were selected and their further separation was performed on a Sephacyl S-400 column. Finally, the major fraction SPF1-1, SPF2-1, and SPF3-1 were collected and lyophilized (Fig. 3-1B-D).

3.3.2. Monosaccharide composition and molecular weight

The chemical composition and molecular weight of three fractions are shown in Table 3-1. Results indicated that three fractions SPF1-1, SPF2-1 and SPF3-1 are acidic polysaccharides with uronic acids of $12.70 \pm 1.80\%$, $26.92 \pm 2.81\%$, and $58.77 \pm 1.64\%$, respectively. The main sugar component of SPF1-1 is glucose. The main neutral sugars of SPF2-1 are arabinose and glucose, and for SPF3-1 are rhamnose (Rha), arabinose (Ara) and galactose (Gal). The protein content of SPF1-1, SPF2-1, and SPF3-1 were low (1.79%, 1.55% and 1.09%, respectively). And the molecular weight (M_w) of SPF1-1, SPF2-1, and SPF3-1 were determined to be 279 kDa, 15.69 kDa, and 13.36 kDa.

3.3.3. UV and FT-IR spectra analysis

The UV spectra of polysaccharide fractions are shown in Fig.3-2. In accordance with protein content in Table 3-1, fractions SPF1-1, SPF2-1, and SPF3-1 were not be detected significant absorption peaks in the wavelength of 280 nm and 260 nm by an ultraviolet spectrophotometer, which indicates that protein and nucleic acid have been reduced to the lowest amount.

The structure of fraction SPFs were identified by FT-IR spectra. As shown in Fig. 3-3, SPF1-1, SPF2-1, and SPF3-1 displayed absorption peaks typical of polysaccharides in the range of $4000-500\text{ cm}^{-1}$. All polysaccharides displayed a broad stretching intense characteristic peak between 3440 and 3422 cm^{-1} , which was the stretching vibration peak of O-H in the sugar molecule. The weak peaks towards $2938-2923\text{ cm}^{-1}$ was belonged to the C-H bond of CH_3 or CH_2 (Hu et al., 2015). The absorption occurring at around $1639-1629\text{ cm}^{-1}$ and $1410-1420\text{ cm}^{-1}$ can be assigned to carboxylate ion stretching band (COO^-), reflecting the existence of uronic acids (Gnanasambanda 2000; Zhang et al., 2013), this result was consistent with the uronic content identified in Table 3-1. The additional peaks at 1737 cm^{-1} and 1248 cm^{-1} in SPF3-1 can be attributed to ester carbonyl (C=O) group and C=O dilatation vibration, which is one of the typical characteristic s of pectin (Wang, et al., 2014). Besides, the peaks at $1024-1035\text{ cm}^{-1}$ and 1079 cm^{-1} were attributed to the arabinofuranose units and galactopyranose from of the backbone of the arabinogalactan. Moreover, the absorption peak at $625-522\text{ cm}^{-1}$ signals that polysaccharide fractions contain α -configurations (Zhao et al., 2017).

3.3.4. NMR analysis

The structure feature of three SPFs were further analysed by the NMR spectra (Fig.3-4) and the signals in ^1H NMR spectra were identified through referring previous

literatures (Huang et al., 2017; Klosterhoff et al., 2018; Shen et al., 2017; Wei et al., 2017; Zhang et al., 2017). The region ranging from δ 3.0-5.5 ppm which were the typical of polysaccharide. The significant signals at δ 5.35, 3.92, 3.89, 3.82, and 3.59 ppm in SPF1-1 could be attributed to \rightarrow 4)- α -Galp-(1 \rightarrow , \rightarrow 6)- β -Galp-(1 \rightarrow , \rightarrow 4)- α -GalpA, \rightarrow 1)- α -GalpA-(4 \rightarrow , and α -Glc(1 \rightarrow 1, respectively (Fig.3-4A). The peak at δ 1.23 ppm in SPF2-1 was assigned to the $-\text{CH}_3$ (C6) of rhamnose, demonstrating the existence of rhamnose. And the anomeric proton at δ 3.58, 3.66, 3.87, 3.99 and 5.29 ppm were attributed to the \rightarrow 1)- α -GalpA-(1 \rightarrow , \rightarrow 6)- β -Galp-(1 \rightarrow , \rightarrow 1)- α -Rhap-(2, 4 \rightarrow , and \rightarrow 4)- α -Galp-(1 \rightarrow , respectively (Fig.3-4B). The anomeric protons at δ 5.15, 5.04, 4.97, and 4.63 ppm in SPF3-1 corresponded with H-1 of anomeric residues α -Araf-(1 \rightarrow , \rightarrow 5)- α -Araf-(1 \rightarrow , \rightarrow 2,4)- α -Rhap-(1 \rightarrow , and α -Rhap-(1 \rightarrow residues, respectively. And at δ 1.31 ppm, it was assigned to the H-6 of α -L-Rhap.

3.3.5. SEM analysis

The polysaccharides isolated in the present study had different textures and surface properties, as revealed using SEM (Fig.3-5). The result show that SPF1-1 was thin porous lamellar structure, SPF2-1 was collective massive structure, and SPF3-1 was fine powdered structure.

3.4. Discussion

In general, the techniques used to extract, purify and separate plant polysaccharides can affect their characteristics (Yu et al., 2017). In this study, three major polysaccharide fractions SPF1-1, SPF2-1, and SPF3-1 were separated and purified from HACP by DEAE Sepharose Fast Flow and Sephacryl S-400 chromatography, yielding 7.4%, 6.9% and 9.8% of the total amount of HACP, respectively. Monosaccharide composition identification indicated that these three isolated fractions are typical pectic polysaccharides which contain similar types of monosaccharide, while they are different in their contents. The size of molecular weight is another critical structural property of polysaccharides, which largely affect its physical and chemical properties. In the present study, the molecular weight of SPF1-1, SPF2-1, and SPF3-1 are 279, 15.69, and 13.36 kD, respectively.

In order to investigate the structure of SPFs fractions, their FT-IR spectrums were recorded from 4000 to 500 m^{-1} using films prepared by the dried polysaccharides and KBr pellets. Results (Fig. 3B) reflect that three polysaccharide fractions have the typical characteristic absorption bands of polysaccharides at 4000-500 cm^{-1} . For instance, all the fractions display a broad stretching peak at around 3440-3422 cm^{-1} for the hydroxyl group,

a weak peak at 2938-2923 cm^{-1} reflects the characteristic absorption of C-H stretching vibration (Hu et al., 2015; Liu et al., 2016). Besides, the absorptions at 1000-1200 cm^{-1} attributed to the ring vibrations overlapped with stretching vibrations of C-OH side groups and the C-O-C glycosidic vibration, suggested the presence of pyranose form of sugars. The difference between SPF1-1, SPF2-1, and SPF3-1 was that SPF3-1 had additional peaks at 1737 cm^{-1} and 1248 cm^{-1} , which were characteristic of ester group and acetyl group, indicated that the GalA units in polysaccharide SPF3-1 was esterified. No significant absorption peak was found at 260-280nm in UV spectrum, implying the absence of protein (Yu et al., 2017). This observation also demonstrates the effectiveness of the fractionation and purification procedures in this study.

Furthermore, NMR was applied to characterize the main structure feature of SPFs. The signals observed in the ^1H spectra of each fraction were assigned based on published values. NMR spectroscopic analysis demonstrated that all of the fractions contained heteropolysaccharides. The ^1H signal at δ 4.70 ppm is due to D_2H . The chemical shifts ranging from δ 3.5–4.5 ppm were attributed to C-2-C-6 protons. SPF1-1 showed the presence of three major anomeric proton signals at δ 5.35, 3.89, and 3.80 ppm, which were assigned as the proton at C-1 for the following structures: $\rightarrow 4)\text{-}\alpha\text{-Galp}-(1 \rightarrow$, $\rightarrow 4)\text{-}\alpha\text{-GalpA}$, $\rightarrow 1)\text{-}\alpha\text{-GalpA}-(4 \rightarrow$. The peaks at δ 1.23 ppm in SPF2-1 and SPF3-1 was assigned to the $-\text{CH}_3$ (C6) of rhamnose, demonstrating the existence of rhamnose. The ^1H signals at δ 5.14/4.98 ppm from SPF3-1 proved that the $\alpha\text{-GalpA}$ was partly methyl esterified (Fig. 3-4C). This was consistent with the FT-IR result in Fig. 3-3C.

3.5. Summary

In this chapter, three major fractions were purified from HACP. SPF1-1, SPF2-1, and SPF3-1 were acidic polysaccharides and differed in molecular weight, monosaccharide composition, and ultrastructure. This study will expand the knowledge of the structural features of polysaccharides from *H. angustifolia*. Further, it can help determine the relationship between the structure of the obtained substances and their useful properties during studies of their physiological and biological activity.

Table 3-1 Chemical composition and molecular weight of SPF1-1, SPF2-1, and SPF3-1

	Carbohydrates	Mw	Uronic acid	Protein	Phenolic compounds	Natural sugar composition (mol%)						
						(wt%)	(kD)	(wt%)	(wt%)	Rha	Glc	Gal
SPF1-1	87.6	279	12.70 ± 1.80	1.79 ± 0.27	5.69 ± 0.35	0.1	92.2	1.1	4	1.1	0.2	1.4
SPF2-1	83.2	15.7	26.92 ± 2.81	1.55 ± 0.03	8.38 ± 0.52	2.6	35.6	14	29.9	3.9	0.5	13.5
SPF3-1	74.8	13.4	58.77 ± 1.64	1.09 ± 0.23	1.01 ± 0.58	22.1	4.5	18.2	37.3	2	1.1	14.8

Rha: Rhamnose, Glc: Glucose, Gal: Galactose, Ara: Arabinose
 Man: Mannose, Fuc: Fucose, Xyl: Xylose

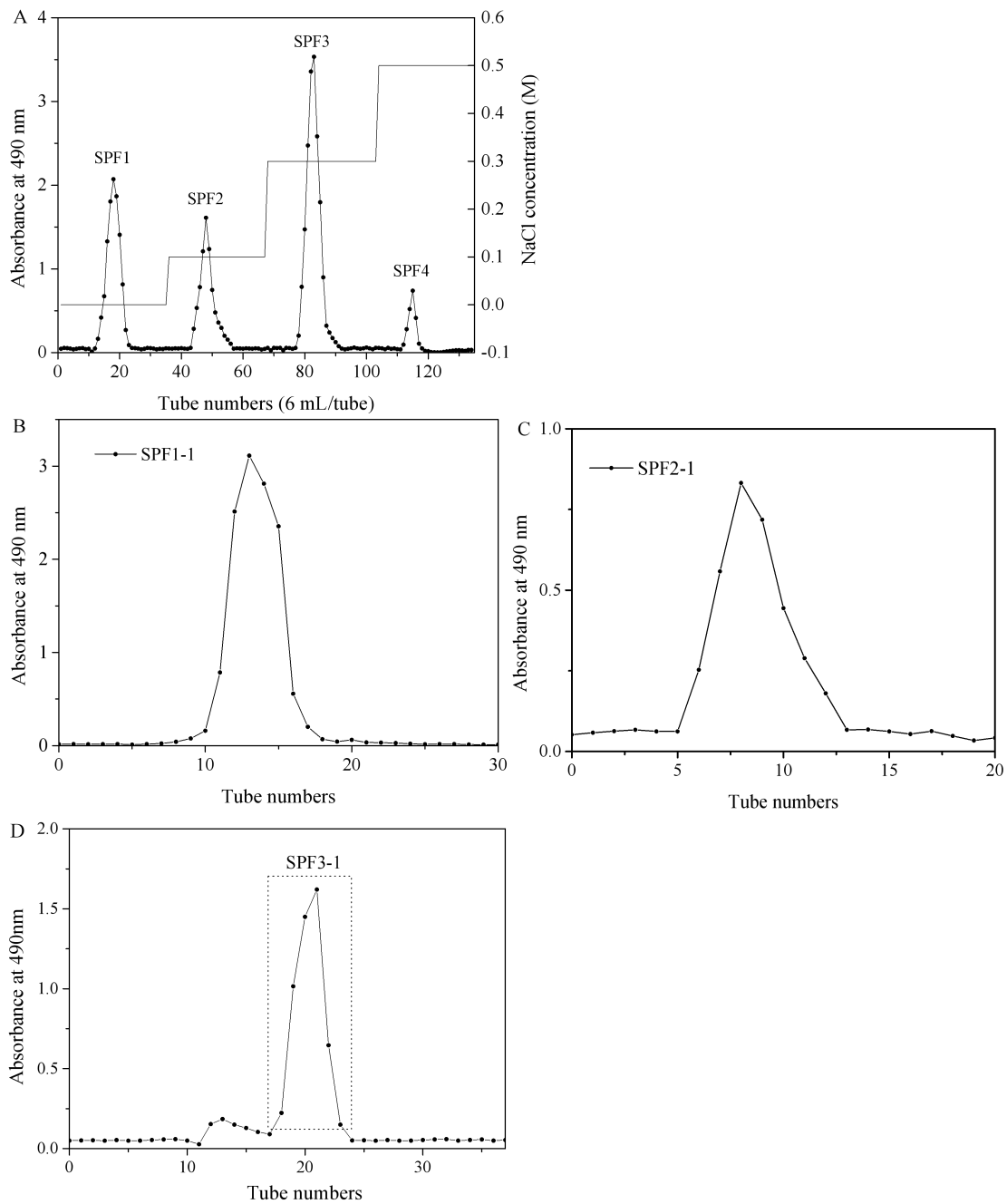


Figure 3-1 Purification and characterization of polysaccharide fractions from HACP

(A) Elution profiles of HACP on the chromatography column DEAE Sepharose Fast Flow;

(B) Elution curve of fraction SPF1-1 on size-exclusion chromatography Sphacryl S-400;

(C) Elution curve of fraction SPF2-1 on Sphacryl S-400; and (D) Elution curve of fraction

SPF3-1 on Sephacry S-400.

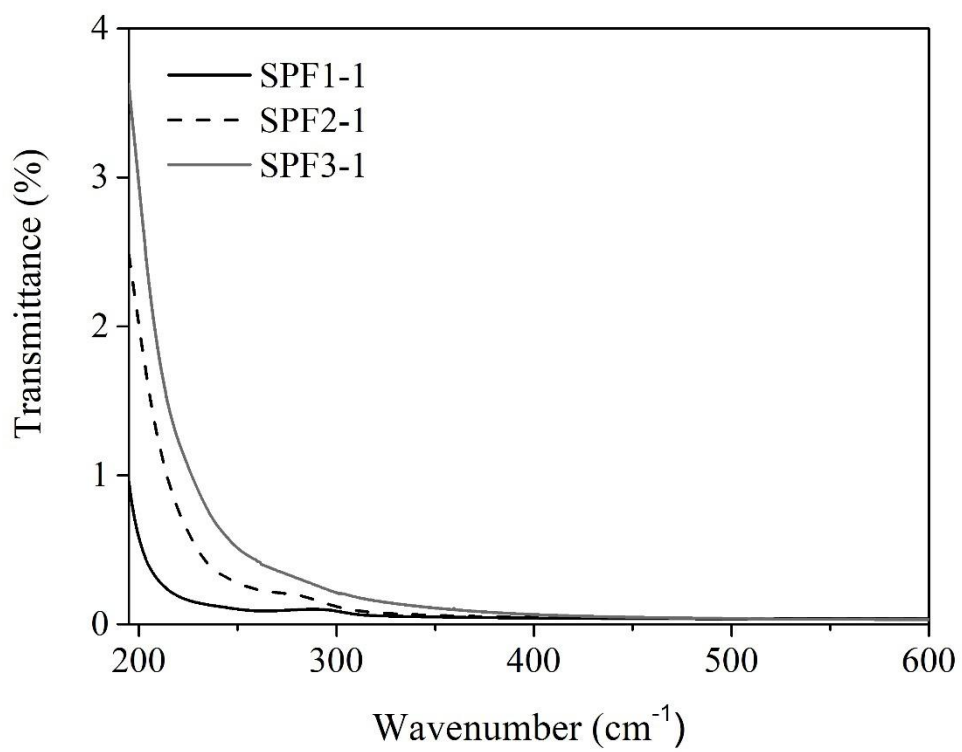


Figure 3-2 UV spectrum of polysaccharide fractions: (A) SPF1-1; (B) SPF2-1; (C) SPF3-1

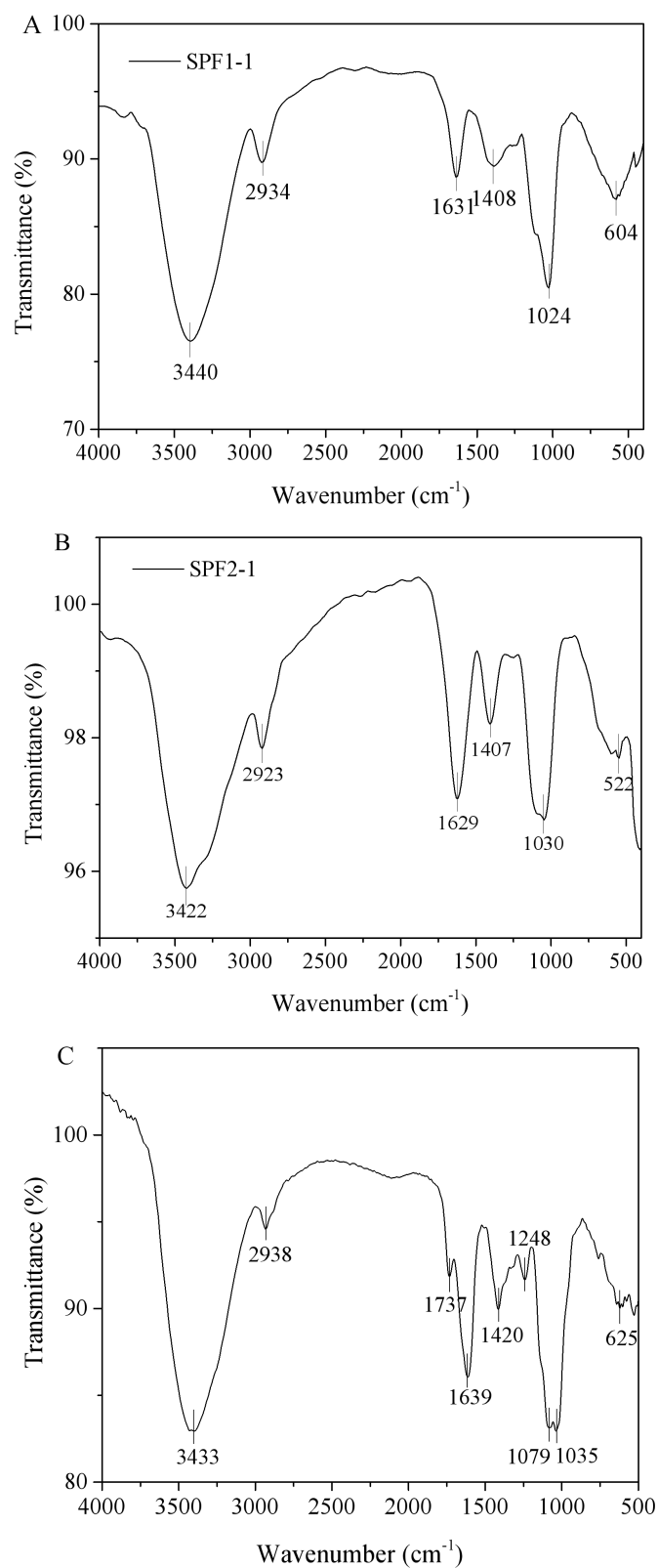


Figure 3-3 FTIR spectrum of polysaccharide fractions

(A) FTIR spectrum of fraction SPF1-1; (B) FTIR spectrum of fraction SPF2-1; and (C) FTIR spectrum of fraction SPF3-1.

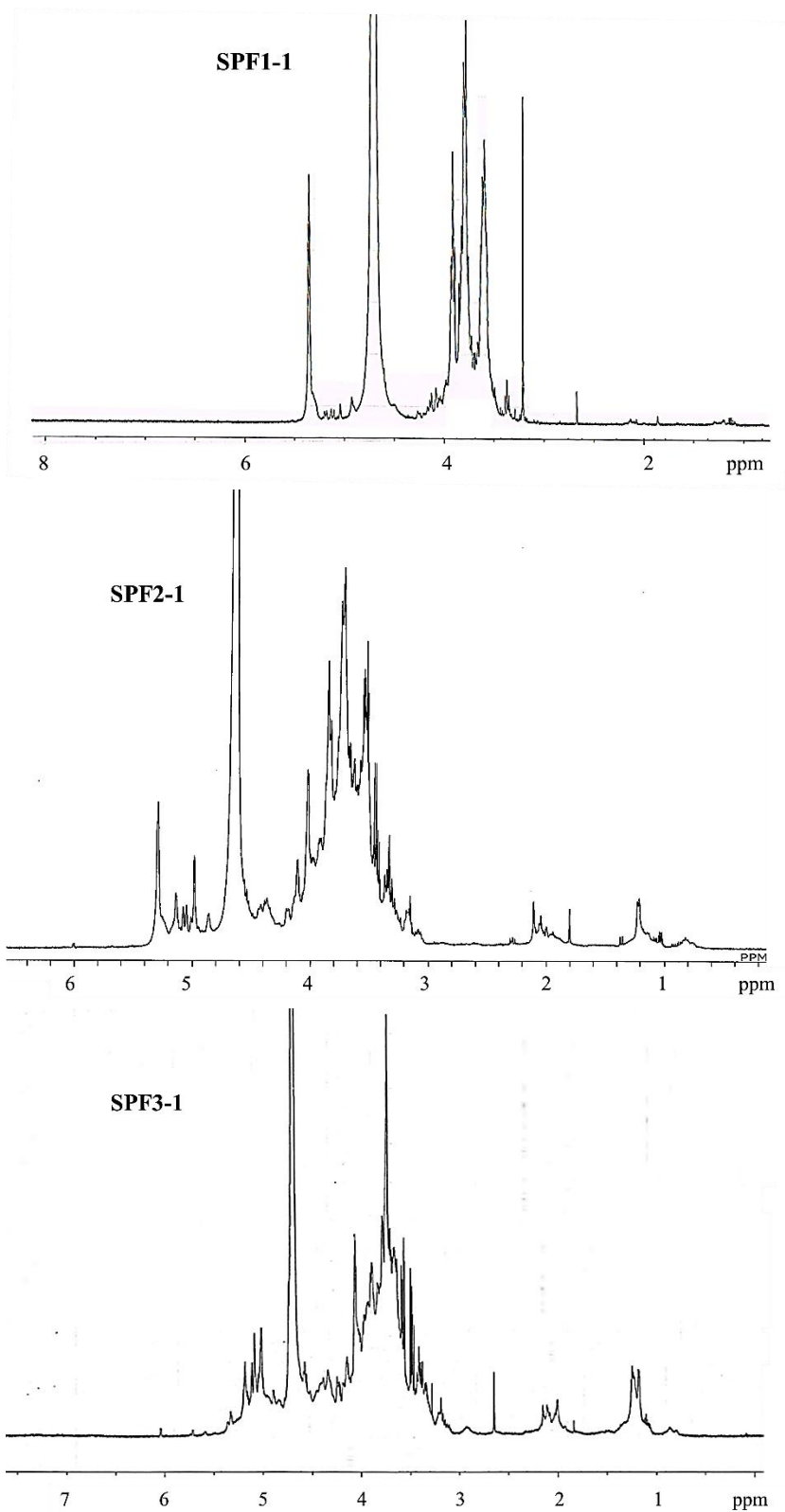


Figure 3-4 ^1H NMR spectrum of polysaccharide fractions

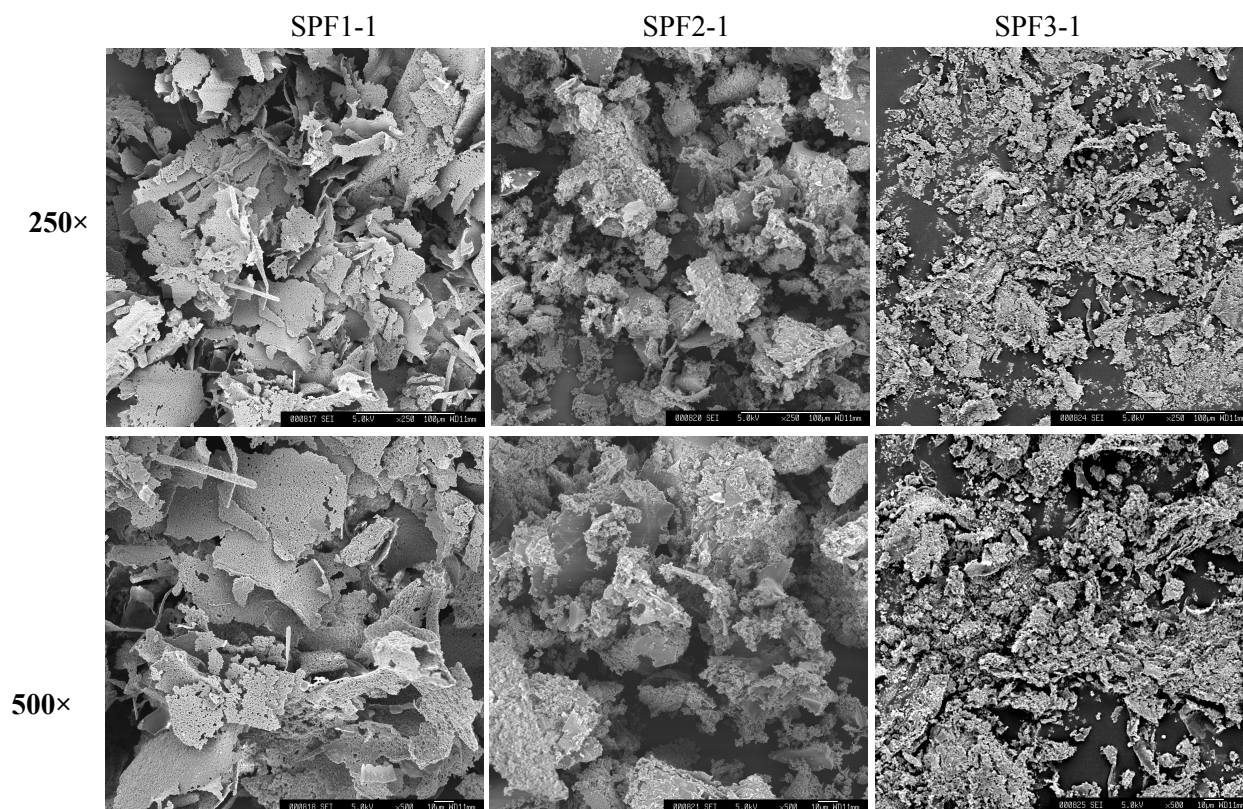


Figure 3- 5 SEM analysis of polysaccharide fractions SPF1-1, SPF2-1, and SPF3-1

Chapter 4 *In vitro* antioxidant and immunomodulatory effects of polysaccharide fractions

4.1. Introduction

Oxidative stress is commonly defined as an imbalance between the production of reactive oxygen species and antioxidant defense. Many disease, such as asthma, inflammation, and diabetes, are thought to be linked to oxidative stress (Atoui et al., 2005; Metcalfe & Alonso-Alvarez, 2010). Antioxidants are defined as the substances which are involved in the prevention of excessive reactive species oxidation at low concentrations (Sarangarajan et al., 2017). Natural antioxidants are reported as a kind of effective free radical scavenger which playing a critical role in protecting body against oxidative stress. Methods used for measuring antioxidants activity of those substances have advanced remarkably during the last few decades. To date, various chemical assays coupled with highly sensitive and automated detection technologies are employed for evaluation of antioxidant activity through particular mechanisms, for example, scavenging activity against certain types of free radicals, reducing power, and metal chelation.

Immunomodulation is regarded as one of the important body's defense against pathogens, inflammatory diseases, and cancer. Our immune system contains several kinds of immune cells. Among them, macrophage cell is important target for studying cellular immunity and molecular immunology, and it is an important cellular bridge between innate and adaptive immunity. In recent years, polysaccharide from natural sources have attracted extensive attention due to their structural diversity, low toxicity and strong antioxidant and immunomodulatory activities. Therefore, discovery and evaluation of polysaccharides with antioxidant and immunomodulatory properties has emerged as one of the important research fields in chemistry and biology and medicine.

4.2. Materials and methods

4.2.1. Chemicals and reagents

Dulbecco's modified eagle medium (DMEM), streptomycin, penicillin and fetal bovine serum (FBS) were obtained from GIBCO (Grand Island, NY, USA). 2, 2'-Azino-bis (3-ethylbenzothiazoline-6-sulfonic acid) (ABTS) and 2, 2-diphenyl-1-picryl-hydrazyl radical (DPPH), Griess reagent, lipopolysaccharide (LPS), 3-(4, 5-Dimethylthiazol-2-yl)-2, 5-diphenyltetrazolium bromide (MTT), and Red blood cell lysis buffer were purchased from Sigma Aldrich, Inc. (Saint Louis, MO, USA). Mouse TNF- α , and IL-6 ELISA Kits

were purchased from eBioscience (San Diego, CA, USA). All the reagents used in this study were of analytical grade.

4.2.2. Antioxidant activity assays

(1) DPPH radical scavenging activity

The DPPH radical scavenging activity of root or leaf extracts were assessed according to a literature with some modifications (Zhang et al., 2015). 2 mL different concentrations (62.5-1000 µg/mL) of the test samples were mixed with 2 mL DPPH (2 mM); the mixture was shaken vigorously and then incubated for 30 min at room temperature at dark place. The OD value was measured at 517 nm using a spectrophotometer. Decrease in absorbance of the DPPH solution indicated an increase of the DPPH radical-scavenging activity. In this study, ascorbic acid was used as the positive control and DPPH radical-scavenging activity was assessed by the following equation:

$$\text{DPPH radical-scavenging activity (\%)} = (1 - A_1 / A_0) \times 100\%.$$

Where, A_1 and A_0 were the absorbance of the sample (tested fractions) and control, respectively.

(2) Hydroxyl radical scavenging activity

The hydroxyl radical scavenging activity was determined according to a literature procedure (Smirnoff & Cumbes, 1989) with some modifications. Different concentration (62.5-1000 µg/mL) of SPFs (100 µL) was mixed with 50 µL of FeSO₄ (1.5 mM), 35 µL of H₂O₂ (60 mM), and 15 µL of sodium salicylate (20 mM). The mixture was mixed thoroughly and incubated at room temperature for 60 min. In this study, Trolox was used as the positive control. The absorbance was measured at 562 nm.

Hydroxyl radical scavenging activity was expressed as a rate (%) and calculated as:

% scavenging of OH• = $[1 - (A_1 - A_2 / A_0)] \times 100\%$, where, A_1 was the absorbance of the sample or ascorbic acid, and A_2 was the absorbance of the reagent blank without sodium salicylate, whereas A_0 was the absorbance of the solvent control, respectively.

(3) ABTS radical scavenging activity

The ABTS radical scavenging activity was measured according to a literature procedure (Debnath et al., 2011) with some modifications. 25 mL of ABTS•+ solution (7mM) was mixed with K₂S₂O₈ solution (140 mM) and stored the mixture in the dark at room temperature for 15-16 h before use. The ABTS•+ solution was diluted with a phosphate buffered saline (PBS, pH = 7.4) to obtain the absorbance to within 0.70 ± 0.02 at

734 nm. Then 0.15 mL of various concentrations (125-2000 µg/mL) of the samples were mixed with 2.85 mL of ABTS•+, and the absorbance was measured at 734 nm after incubation at room temperature for 10 min.

The scavenging activity of ABTS free radical was calculated by the following equation:

$$\text{ABTS scavenging activity (\%)} = (C - D) - (A - B) / (C - D) \times 100$$

Where, A = absorbance of ABTS solution + sample/standard, B = absorbance of PBS + sample/standard, C = absorbance of ABTS solution + distilled water, and D = PBS + distilled water.

(4) Reducing power

The reducing power of tested samples was measured according to a literature procedure (Li et al., 2015). Different concentrations (250-4000 µg/mL) of sample solution (1 mL) was mixed with 1 mL of phosphate buffer (200 mM, pH 6.6), and 1mL of 1% potassium hexacyanoferrate [K₃Fe (CN)₆], the mixture was then incubated for 20 min using a water bath at 50°C. After incubation, 1mL of 10% trichloroacetic acid (TCA, w/v) was added, and then centrifuged at 1500 rpm/min for 10 min. The supernatant (2 mL) was mixed with 2 mL of distilled water and 0.4 mL of 0.1% ferric chloride (FeCl₃). Finally, the absorbance was measured at 700 nm using a spectrophotometer. A higher absorbance means a higher reducing power activity. In this study, Trolox was used as the positive control.

(5) Ferrous ion chelating activity

The ferrous ion chelating ability of samples was investigated as reported previously (Kalın, Gülçin, & Gören, 2015) with modifications. Samples (50 µL) in various concentrations were mixed with FeSO₄ (100 µL, 0.13 mM) and the reaction was performed by adding 50 µL ferrozine (2.0 mM) to the mixture. The mixture was left standing for 10 min at 25°C and then the absorbance at 562 nm was detected. Ethylene diamine tetraacetic acid disodium salt (EDTA-2Na) was used as the positive control.

The ferrous ion chelating activity was estimated by the following equation:

$$\text{Fe}^{2+} \text{ chelating activity (\%)} = [1 - A_1 - A_2 / A_0] \times 100$$

where deionized water was used as the blank control. A₀ was the value of the absorbance, A₁ was the absorbance of the reaction system, containing both test sample and reaction solution, and A₂ was the absorbance of the test sample only with deionized water instead of reaction solution.

(6) Superoxide anion radical scavenging activity

Superoxide anion radical scavenging activity of polysaccharide fractions was based on the method described by (Chidewe et al., 2016). 1 mL of nitroblue tetrazolium (NBT) solution (156 μ M NBT in 100 mM phosphate buffer, pH 7.4) was mixed with 1 mL of NADH solution (468 μ M NBT in 100 mM phosphate buffer, pH 7.4) and 1 mL of polysaccharide solutions (31.25-1000 μ g/mL). The reaction then started by adding 100 μ L of phenazine methosulphate (PMS) solution (60 μ M PMS in 100 mM phosphate buffer, pH 7.4) to the mixture. The reaction mixture was incubated at 25°C for 5 min and the absorbance at 560 nm was measured against blank sample. Decreased absorbance of the reaction mixture indicated increased superoxide anion scavenging activity. The percentage inhibition of superoxide anion generation was calculated using the formula:

$$\% \text{ inhibition of superoxide anion} = [(A_0 - A_1) / A_0] \times 100.$$

Where A_0 is the absorbance of the control, and A_1 is the absorbance of the sample or standard.

4.2.3. Cell line and culture

Human fibrosarcoma cell line HT1080 were obtained from Riken Cell Bank (Tsukuba, Japan), and cultured with DMEM supplemented with 10% FBS, penicillin (100 U/mL) and streptomycin (100 μ g/mL) at 37°C in an incubator with 5% CO₂ atmosphere.

4.2.4. Cytotoxicity of SPF3-1

The effects of SPF3-1 on HT1080 cell viability were identified by using MTT assay according to Li et al. (2016). Cells (5000 cell/well) were treated with/without virous concentrations of polysaccharide fractions (6.25-400 μ g/mL) for 24 h. The optical density at 450 nm was measured by using a Model 550 microplate reader (BIO-RED, Tokyo, Japan).

4.2.5. *In vitro* immunomodulatory activities

(1) Macrophages proliferation activity

Briefly, RAW264.7 cells were suspended in DMEM and adjusted to a concentration of 5×10^4 cells/mL. One hundred microliters cell solutions were loaded onto 96-well culture plates and cultivated overnight, and then treated with polysaccharide samples at different concentrations (6.25-100 μ g/mL) for 24 h. Cells treated with DMEM medium only was used as blank control. After incubation, cell viability was determined by CCK-8 assay.

(2) Phagocytic activity determination

The phagocytic uptake ability of macrophages was measured according to the method described previously (Li et al., 2016) with some modifications. Macrophages were pre-incubated in 96-well plates for 12 h and then treated without/with polysaccharide fractions at various doses (6.25-100 µg/ml) for 24 h, followed by addition of 100 µL of neutral red (0.7%, w/v) and cultivation at 37°C for 1 h. Finally, the medium was discarded, and the cells were washed with cold PBS for three times. Afterwards, cell lysis buffer (1% glacial acetic acid: ethanol = 1:1, 100 µL/well) was added and the cells were incubated at room temperature (25 ± 2°C) for another 1 h, and then the optical density at 540 nm was measured by using a microplate reader.

(3) Measurement of the nitric oxide (NO) production

RAW 264.7 cells (1×10^5 cells/well) were cultured in 48-well plates and stimulated with or without various doses of samples (6.25-100 µg/mL). LPS (10 µg/mL) was used as the positive control. After 24 h of incubation, the culture supernatant was collected, and NO level was measured by using Griess reagent assay (Li et al., 2017).

(4) Protective activity on doxorubicin (DOX)-induced damage

RAW 264.7 cells were seeded in a 96-well plate at 5×10^3 cells/well. After 24 h of adherence, cells were treated with DOX (0.5 µmol/L, final concentration) in the absence or presence of various concentrations (6.25-100 µg/mL) of SPFs for 24 h. Cell viability was determined using CCK-8 method.

(5) Analysis cytokines release in culture medium

RAW 264.7 cells were treated with SPF3-1 (6.25-100 µg/mL) for 24 h. The cytokines TNF- α , and IL-6 released in culture supernatant were determined by the mouse TNF- α , and IL-6 ELISA Ready-SET-Go reagent sets (eBioscience, San Diego, USA) ELISA Kits according to the instruction of manufacturers. Briefly, an ELISA plate was coated with the capture antibody overnight at 4°C and then filled successively with block solution for 1 h. Next, assay dilution (blank), standards, and samples (culture supernatant) were incubated for 2 h, and this was followed by incubation with antibody detection for 1 h at room temperature. Finally, substrate and stop solution were added to each well, and the optical density was measured at 450 nm. The cells treated with LPS (10 µg/mL) were used as the positive control, and those cultured in DMEM medium in the absence of SPF3-1 and LPS were used as the negative control.

(6) Macrophage-mediated cytotoxicity

The macrophage-mediated cytotoxicity was identified according to Mao et al. (2015)

and Wang et al. (2016) with some modifications. RAW264.7 cells were plated in 24-well plate (2×10^5 cells/well) for 24 h of adherence, followed by LPS (10 $\mu\text{g}/\text{mL}$) or various concentrations of SPF3-1 treatment. The cells without any treatment was used as the control group. After 24 h, the supernatant and adherent cells were collected individually. Then, the supernatants were added to a 96-well plate containing adherent HT1080 cells (target cell: 4×10^3 cells/well) and cultured for 48 h. HT1080 cell viability was identified by using MTT assay. Simultaneously, 100 μL of the above SPF3-1 pre-activated macrophage cells (effector cells, 2×10^5 cells/mL) were co-incubated with 100 μL of adherent HT1080 cells (target cells, 2×10^4 cells/mL) for 48 h. The HT1080 cells co-incubated with macrophage cells which without SPF3-1 treatment was used as negative control group, and cells cultured with LPS pre-activated macrophages was used as positive control. The cell viability was calculated by using the following equation: HT1080 cell activity (%) = $100 \times (\text{OD}_T - (\text{OD}_S - \text{OD}_E)) / \text{OD}_T$, where OD_T means the optical density of target cells control, OD_S is the optical density of tested sample, and OD_E is the optical density of the effector cells control.

(7) Spleen lymphocytes proliferation and cytokines generation assay

Spleen lymphocytes were isolated from BALB/c mice as described in 2.2.9, chapter 2. Lymphocytes were seeded into 96-well plates at a density of 5×10^5 cells per well. SPF3-1 was added at the indicated concentrations, ranging from 6.25 to 100 $\mu\text{g}/\text{mL}$, and incubated for 48 h. Cell viability was identified by using CCK-8 kit.

In order to identify the cytokines produced by SPF3-1 treated lymphocytes, cells were seeded into 96-well plates at a density of 1×10^6 cells per well. SPF3-1 was added at various concentrations ranging from 6.25 to 100 $\mu\text{g}/\text{mL}$ and incubated for 24 h. Then, the culture supernatants were collected, and cytokine quantification of IFN- γ and IL-6 was performed using ELISA kits according to the manufacturer's instructions.

4.2.6. Statistical analysis

All the data were expressed as means \pm standard deviation (SD), and the results used in this work were from at least three independent experiments performed in triplicate. In addition, the statistics were analysed using one-way analysis of variance (ANOVA) with the Duncan's multiple-range test. $*p < 0.05$, $**p < 0.01$, and $***p < 0.001$ were considered as statistically significant.

4.3. Results and discussion

4.3.1. *In vitro* antioxidant activities

(1) Scavenging ability on DPPH radicals

The DPPH radical scavenging assay is a common method that has been widely used to determine the free radical scavenging activity of natural antioxidant. DPPH radical is a stable free radical and has purple color in ethanol solution. Once an antioxidant was added to this system, DPPH radical could easily accept hydrogen atom donated by antioxidant to become a stable molecule which result in a purple colour erosion. The decrease of the color absorption indicates a higher DPPH radical scavenging ability. In the present research, the DPPH radical scavenging activity of SPF1-1, SPF2-1, and SPF3-1 are shown in Fig.4-1A. The scavenging ability against DPPH radical of SPF3-1 increased significantly with the increasing concentration. When the concentration approached to 1000 $\mu\text{g/mL}$, the scavenging rate of SPF3-1 was 74.59%, obviously higher than fractions 1-1 and 2-1 (24.02% and 33.04%, respectively).

(2) Hydroxyl radical scavenging assay

The hydroxyl radical is the most active among oxygen radicals and induces severe oxidative injury to the adjacent bio-molecular. Hence, removing hydroxyl radical is important for the protection of living systems. As shown in Fig. 4-1B, the scavenging activity of SPFs on hydroxyl radical improved with the increase of concentration which exhibits a dose dependent manner. SPF3-1 has showed highest inhibition activity against hydroxyl radical, followed by SPF2-1 and SPF1-1.

(3) ABTS radical scavenging ability

The ABTS radical scavenging assay is extensively applied to measure the total antioxidant power of compounds extracted from various plants. The ABTS radical scavenging potentials of SPF1-1, SPF2-1, and SPF3-1 are presented in Fig. 4-1C. Result demonstrates the concentration dependent increase of ABTS radical scavenging activities of SPFs. And SPF3-1 exhibited higher ABTS radical scavenging ability at all concentrations tested. The maximum inhibition ability (10.2%, 23.6%, and 57.4%) of SPF1-1, SPF2-1 and SPF3-1 were obtained at the concentration of 2000 $\mu\text{g/mL}$, which is clear that SPF3-1 showed highest ABTS radical scavenging activity.

(4) Reducing power

Reducing power assay always be served as a significant indicator of potential antioxidant activity of samples. As shown in Fig. 4-1D, the reducing potential of SPF1-1, SPF2-1, and SPF3-1 increased to 0.14, 0.27 and 0.66, respectively as the concentrations increased to 4000 $\mu\text{g/mL}$. However, the positive control trolox showed a stronger reducing

power (1.36 at 4000 µg/mL) than the polysaccharides examined. These results indicated that SPF3-1 exhibited a stronger reducing power than SPF1-1 and SPF2-1 and should be explored as potential antioxidants.

(5) Ferrous ion (Fe²⁺) chelating capacity assay

Iron induces the formation of free radical by catalysing the conversion of superoxide radical to toxic hydroxyl radical. As shown in Fig. 4-1E, SPFs have displayed significant ferrous ion chelating activity in a dose dependent manner. SPF1-1 and SPF2-1 showed a relatively moderate ability to chelate Fe²⁺ (29.6% and 38.8%), while SPF3-1 exhibited a stronger chelating capacity accounting for 63.2% at the concentration of 4000 µg/mL.

(6) Superoxide radical inhibition assay

Superoxide radical is known to produce precursors of hydroxyl radical *in vivo*, causing damage to DNA and membrane of cell. Therefore, scavenging ability of superoxide radical is extremely important to antioxidant research. The superoxide radical scavenging activity of the obtained polysaccharide fractions and Trolox (VE) were evaluated and shown in Fig. 4-1F. At a concentration of 62.5-1000 µg/mL, the SPFs exhibited varying degrees of antioxidant activities with a concentration-dependent manner. Compared to SPF3-1, SPF1-1 and SPF2-1 had lower levels of superoxide radical scavenging activities. The highest ability of SPF1-1 (28.7%) and SPF2-1 (46.4%) were obtained at concentration of 1000 µg/mL. Whereas the inhibition ratio of SPF3-1 reached to 57.5% at the same tested concentration, significant higher than SPF1-1 and SPF2-1.

4.3.2. *In vitro* immunomodulatory activities

(1) Macrophages proliferation effect

Macrophage cell is one of the most important immune cells of innate immune system, always act as the first effector cell to aging cells, pathogens and cancer cells (Sun et al., 2015). The activation of macrophages has been considered as a primary and necessary step for immune system stimulation. In the present study, the macrophage cell activation ability of SPFs was first identified by MTT assay. According to Table. 4-1, the macrophage cell proliferation of all SPFs-treated groups was significantly stronger than that of blank control and exhibited remarkable concentration-dependent characteristics. Different with SPF1-1 and SPF2-1, fraction SPF3-1 showed obvious stronger macrophages proliferation effect at all the concentrations tested, indicating that SPF3-1 may exhibits higher immunomodulatory activity.

(2) Effects of SPFs on macrophages phagocytosis and NO production

One of the most distinguished features of macrophage activation would be an increase in phagocytic activity. In the present study, the immunomodulatory effects of purified fractions on the phagocytosis of macrophages *in vitro* were investigated by the uptake of neutral red. As shown in Fig. 4-2A, all the fractions significantly enhanced macrophage phagocytosis to various degree in the dose range of 6.25-100 $\mu\text{g}/\text{mL}$, indicated that all the polysaccharide samples had the abilities to activate macrophages. Obviously, SPF3-1 showed higher phagocytosis stimulating ability, and the extent of stimulation followed the order SPF3-1 > SPF2-1 > SPF1-1.

As a kind of important molecules produced by macrophages, NO plays a vital role in the regulation of apoptosis and host defence against pathogens and tumor cells. At the same time, NO could also enhance the lysis and phagocytosis of macrophages. Thus, the ability to release NO by macrophages reflects the effects of polysaccharides on immune function. In this work, a significant increase was detected in NO release in various SPFs treated macrophages in a dose-dependent manner (Fig. 4-2B). Particularly, the NO production was $10.40 \pm 0.56 \mu\text{M}$ at 100 $\mu\text{g}/\text{mL}$ of SPF3-1 treated group, significantly higher than the SPF1-1 and SPF2-1 group (6.98 ± 0.28 and $8.23 \pm 0.39 \mu\text{M}$).

(3) Protection effect of SPFs on DOX-induced cytotoxicity

DOX always used for cancer treatment, and it has been demonstrated to cytotoxic to macrophage cell (Li et al., 2016). As shown in Fig. 4-2C, treatment with 0.5 $\mu\text{mol}/\text{L}$ DOX decreased the survival rate of RAW 264.7 cells to 39.58%. While in the presence of SPFs, the cell viability of RAW 264.7 was significantly increased, reaching to the maximum (83%, 86%, and 98%) at SPF1-1, SPF2-1, and SPF3-1 concentration of 100 $\mu\text{g}/\text{mL}$, respectively.

(4) Measurement of SPF3-1 on cytokines production of macrophage cells

Cytokines are small molecular proteins secreted by activated macrophages. They can mediate and regulate immune response against tumor growth. Among them, TNF- α is a cytokine which has been recognized as an important host regulatory molecule with tumor necrosis activity. In addition, as an important regulator of host defense responses, IL-6 contributes to the pathogenesis of various inflammatory and immunologic diseases, also can produced by activated macrophages. In the present study, according to Fig. 4-3A, the TNF- α release in the untreated control group was low ($97.46 \pm 5.40 \text{ pg}/\text{mL}$), while the treatment with 6.25 $\mu\text{g}/\text{mL}$ of SPF3-1 resulted in one-fold increase in TNF- α production compared with the control group. The highest level of $336.82 \pm 4.63 \text{ pg}/\text{mL}$ was obtained

in 100 µg/mL SPF3-1 treated group, exhibiting no significant difference with the positive LPS control (356.33 ± 12.64 pg/mL). SPF3-1 also remarkably induced the release of IL-6 in a dose dependent manner at concentrations of 12.5-100 µg/mL (Fig. 4-3B). These results suggest that SPF3-1 could significantly stimulate the macrophages immune response *via* the release of NO and cytokines TNF- α and IL-6.

(5) Cytotoxic effect of SPF3-1 treated macrophages on HT1080 cells

As seen in Fig. 4-4A, the macrophages induced by SPF3-1 significantly reduced the cell proliferation of HT1080 cells when compared with the control group ($p < 0.01$). The maximum inhibition effect ($41.5 \pm 2.8\%$) was determined at 100 µg/mL of SPF3-1 treated group, even higher than the positive LPS group ($30.1 \pm 2.1\%$), greatly in agreement with the above observation on the resultant enhanced macrophages immune response and phagocytosis capacity against cancer cells after pretreatment with SPF3-1. Meanwhile, co-incubation with culture media from SPF3-1 treated macrophages resulted in a significant reduction in cell viability of HT1080 cells (Fig. 4-4B). The above results demonstrate that after pre-treatment with SPF3-1, the macrophages and culture media possessed a cytotoxic activity against HT1080 cells. No direct cytotoxic effect of SPF3-1 on HT1080 cell was detected in this work (Fig. 4-4C), indicating that SPF3-1 exhibits an indirect cytotoxicity on HT1080 cancer cells probably by stimulating macrophages immune response.

(6) Effects of SPF3-1 on splenic lymphocyte proliferation and cytokines generation

The immunological activities of SPF3-1 was further investigated by testing its effects on lymphocyte proliferation *in vitro*. As shown in Fig. 4-5, SPF3-1 application strongly promoted the lymphocytes proliferation ($p < 0.05$) in the concentration ranging from 6.25 to 100 µg/mL, which exhibited a dose dependent manner. The highest viability of lymphocyte increased to 195.9% after 100 µg/mL of SPF3-1 treatment for 48h, indicating its potent lymphocyte activation strategy.

In the present study, the effects of SPF3-1 on mouse lymphocytes IL-6 and IFN- γ were determined with results shown in Fig. 4-6. Clearly, SPF3-1 treatment efficiently promoted lymphocytes IL-6 and IFN- γ release. At concentration of 100 µg/mL, IL-6 and IFN- γ production increased to 117.3 ± 25.7 pg/mL and 63.6 ± 8.3 pg/mL, significantly higher than the control groups (36.8 ± 1.4 pg/mL and 21.0 ± 3.3 pg/mL).

4.4. Discussion

In this study, *in vitro* antioxidant activities of separated polysaccharide fractions were evaluated by detection of DPPH radical, ABTS radical, hydroxyl radical and superoxide radical scavenging activity, as well as reducing power and ferrous ion chelating activity. Results reflect that SPF3-1 exhibited higher antioxidant activities, followed by SPF2-1 and SPF1-1. It is widely believed that the bioactivities of polysaccharides are affected by their structure characteristics, such as monosaccharide composition, molecular weight, and chain conformation (Sun et al., 2018). Previous study demonstrated that DPPH radical scavenging activity showed significant correlations with arabinose content and galactose content (Zhang et al., 2018). In this study, SPF3-1 contents significant arabinose and relative higher galactose exhibited strongest DPPH radical scavenging effects. In addition, the higher galactose and xylose amounts in SPF2-1 and SPF3-1 were found highly correlated with reducing power and metal chelating activity, this is also confirmed by a previous study (Zhang et al., 2018).

Molecular weight was one of the most important structure features of polysaccharide. A number of reports suggested that the antioxidant activity of polysaccharides was also influenced by Mw. It was supposed that low molecular weight polysaccharides had strong antioxidant activity (Siu et al., 2016). In the present study, SPF2-1 and SPF3-1 with lower molecular weight possessed better performances in antioxidant assays, while SPF1-1 had the highest molecular weight exhibited relatively lowest antioxidant abilities. Generally, the acidic polysaccharides, which contained a certain amount of uronic acid, were potent antioxidants. In the present study, SPF3-1 with highest uronic acid content (58.77%), exhibited strongest antioxidant activities, followed by SPF2-1 (26.92%), and SPF1-1 (12.70%). In summary, this study inferred that the molecular weight, and uronic content have influences on the antioxidant activity of *H. angustifolia* polysaccharides, resulting from SPF3-1 with moderate molecular weight, and highest uronic content exhibited strongest antioxidant activities.

Phagocytosis is one of the primary features for macrophages response to pathogens and cancer cells (Liu et al., 2016). Analysis of the phagocytosis capacity of activated macrophages can reflect the effects of sample on immune function. In the present study, polysaccharides SPFs were found to significantly enhance the phagocytosis of macrophages at concentration ranging from 12.5 to 100 $\mu\text{g}/\text{mL}$. Particularly, the resultant OD value after treatment with 100 $\mu\text{g}/\text{mL}$ of SPF3-1 was 0.64 ± 0.04 , almost 2 times of the control group (Fig. 4-2). NO generated by activated macrophages has been identified as

one of the major effector molecules for the destruction of tumor cells. In this work, a significant increase in NO release was detected in various SPFs treated macrophages, which shows a dose-dependent manner (Fig. 4-2B). The NO production was 6.98, 8.23 and 10.4 μM at 100 $\mu\text{g}/\text{mL}$ of SPF1-1, SPF2-1, and SPF3-1 treated group, significantly higher than the control group (3.9 μM). Since SPF3-1 exhibited highest macrophages activate activity, SPF3-1 was selected for further immunomodulatory assay identification. According to Fig. 4-3, the SPF3-1 remarkably induced the release of IL-6 and TNF- α in a dose-dependent manner.

The immunomodulatory activity of polysaccharides on macrophages is usually correlated with its structure, monosaccharides composition and molecular weight. Previous results suggest that polysaccharides are mainly composed of Ara, Xyl, and Gal, and high content of uronic acid plays a positive role in the stimulation of macrophages (Chen et al., 2006; Lo et al., 2007; Sun et al., 2015). In this research, SPF3-1 contains highest molar proportion of Ara (37.3%), Gal (18.2%), Xyl (14.8%) and uronic acid (58.77%, wt%), SPF3-1 was found to strongly stimulate macrophages immune response. In addition, polysaccharides from natural plants with lower molecular weight was proven to possess higher immunomodulatory activities (Xu et al., 2009). In this work, the molecular weight of SPF3-1 was about 13.36 kDa. Therefore, the significant immunomodulatory towards macrophage cells of SPF3-1 is most probably attributable to its small molecular weight, and high contents of Ara, Man, Gal, and uronic acid.

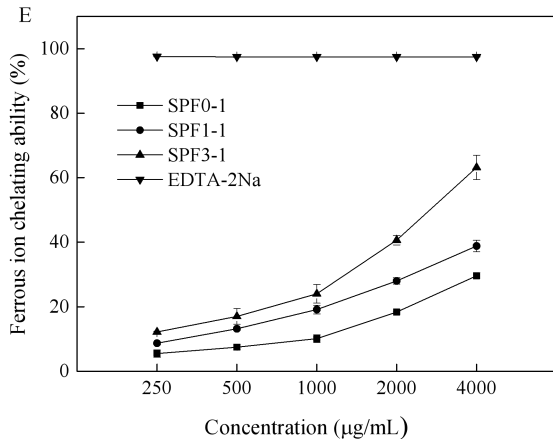
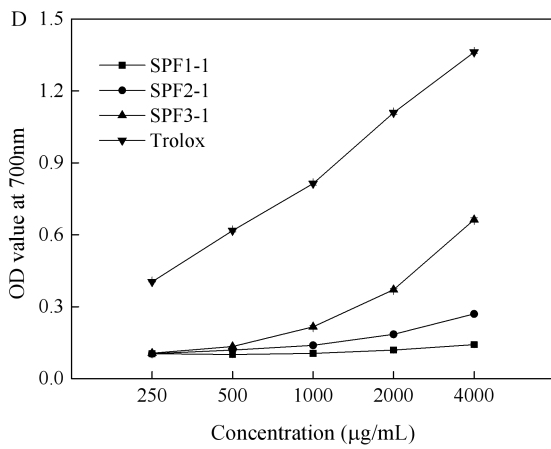
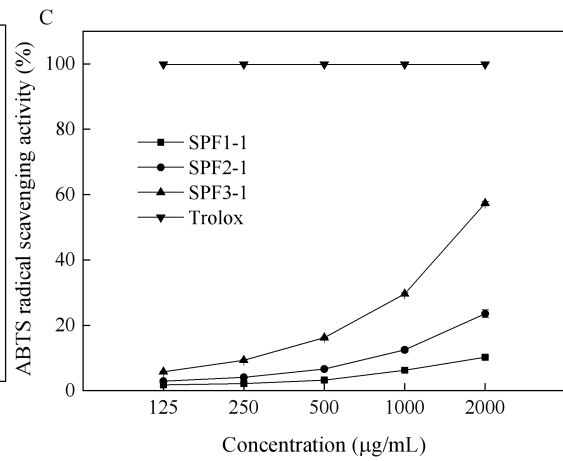
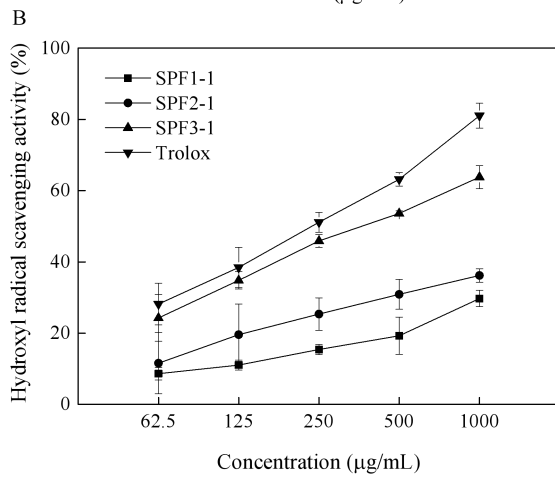
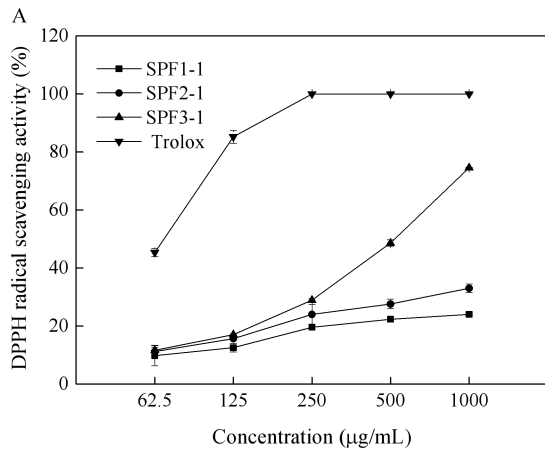
4.5. Summary

All the above findings suggest that fraction SPFs possessed immunomodulatory and antioxidant activities in certain assays. And the potency of their antioxidant and immunomodulatory effects can be ordered SPF3-1 > SPF2-1 > SPF1-1. These results indicated that fraction SPF3-1 has high-efficiency therapeutic antioxidant and immunomodulatory properties and can be utilized as a new source for functional foods or drugs.

Table 4-1 Macrophage cell proliferation ability (%) of polysaccharide fractions from HACP

	Control	6.25 µg/mL	12.5 µg/mL	25 µg/mL	50 µg/mL	100 µg/mL
SPF1-1	100 ± 3.56	136 ± 4.75	143 ± 7.25	150 ± 9.75	153 ± 5.88	157 ± 4.52
SPF2-1	100 ± 5.25	141 ± 2.68	153 ± 5.61	156 ± 3.54	159 ± 4.95	164 ± 4.56
SPF3-1	100 ± 2.77	155 ± 4.85	169 ± 3.31	172 ± 4.80	183 ± 1.45	193 ± 5.62

Results are represented as mean ± SD, *n* = 5.



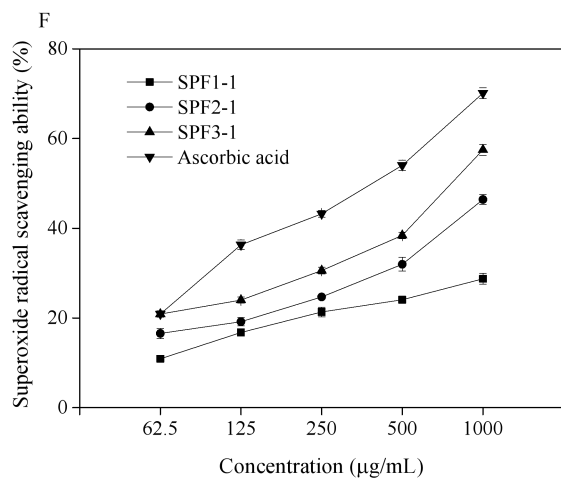


Figure 4- 1 Antioxidant activities of polysaccharide fractions separated from HACP (A) DPPH radical scavenging activity; (B) Hydroxyl radical scavenging ability; (C) ABTS radical scavenging activity; (D) Reducing power; (E) Ferrous ion chelating ability; and (F) Superoxide radical scavenging ability.

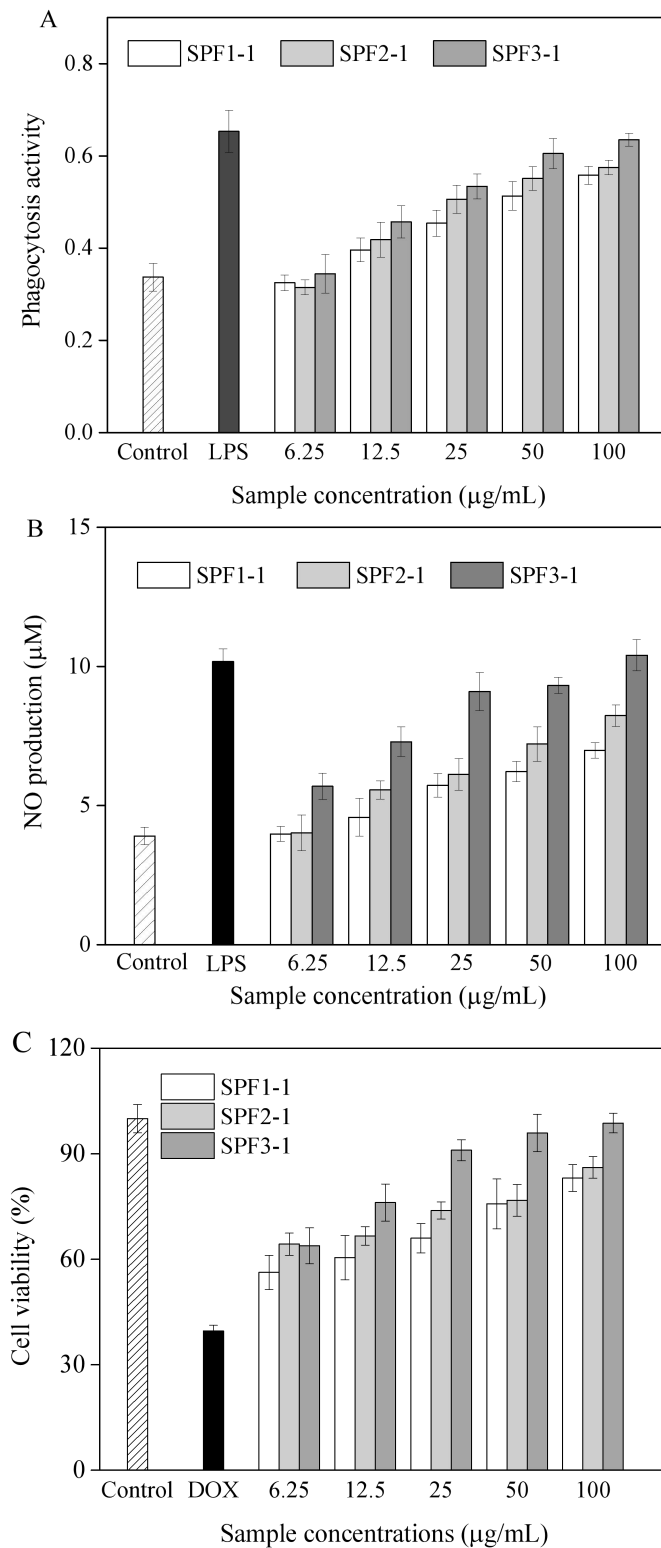


Figure 4-2 Activation effects of SPFs on RAW264.7 cells

(A) Effects on macrophages cell phagocytosis activity; (B) Effects of SPFs on macrophages NO production; and (C) Protection effect on DOX-induced cytotoxicity. The cells were treated with various concentrations of SPFs or LPS (10 μg/mL) for 24 h. Results are represented as mean ± SD, $n = 5$.

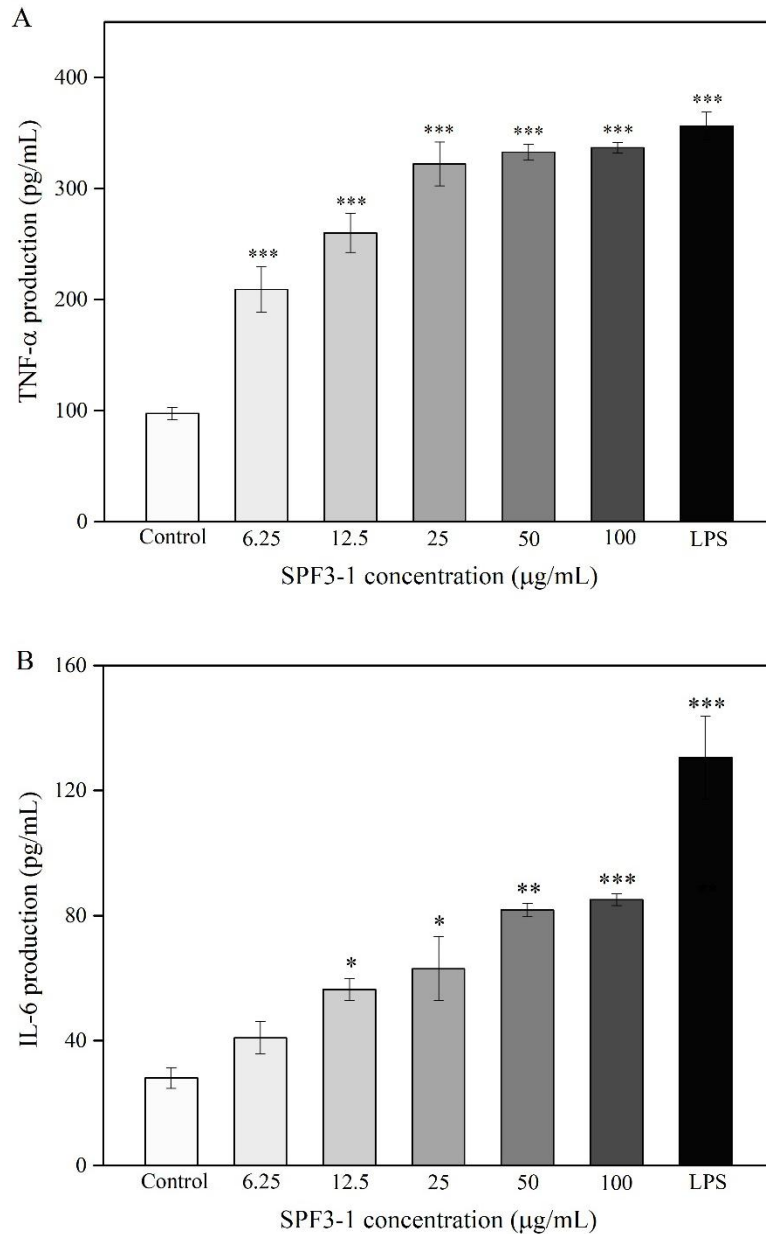


Figure 4-3 Production of cytokines of macrophage cells treated by SPF3-1

(A) TNF- α production; (B) IL-6 levels of culture supernatant from SPF3-1 treated macrophages. Results are represented as mean \pm SD, $n = 5$. * $p < 0.05$, ** $p < 0.01$, and *** $p < 0.001$ denote statistically significant difference between the treated and control groups.

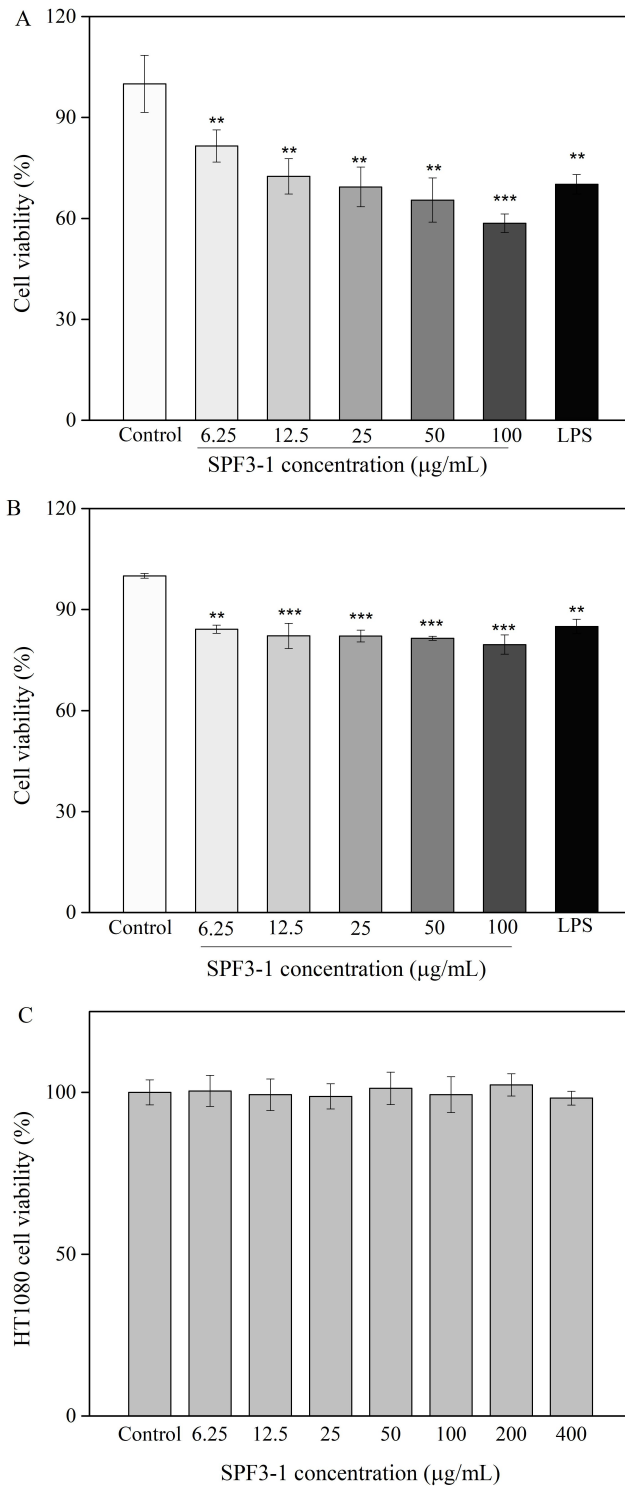


Figure 4-4 SPF3-1 induced cytotoxicity of macrophages against HT1080 tumor cells (A) Cytotoxicity of SPF3-1 activated RAW264.7 towards HT1080 tumor cells; (B) Cytotoxic effect of culture supernatant from SPF3-1 treated macrophages; and (C) Effects of SPF3-1 on HT1080 cell viability. Results are represented as mean \pm SD ($n = 5$). * $p < 0.05$, ** $p < 0.01$, and *** $p < 0.001$ denote statistically significant difference between the treated and control groups.

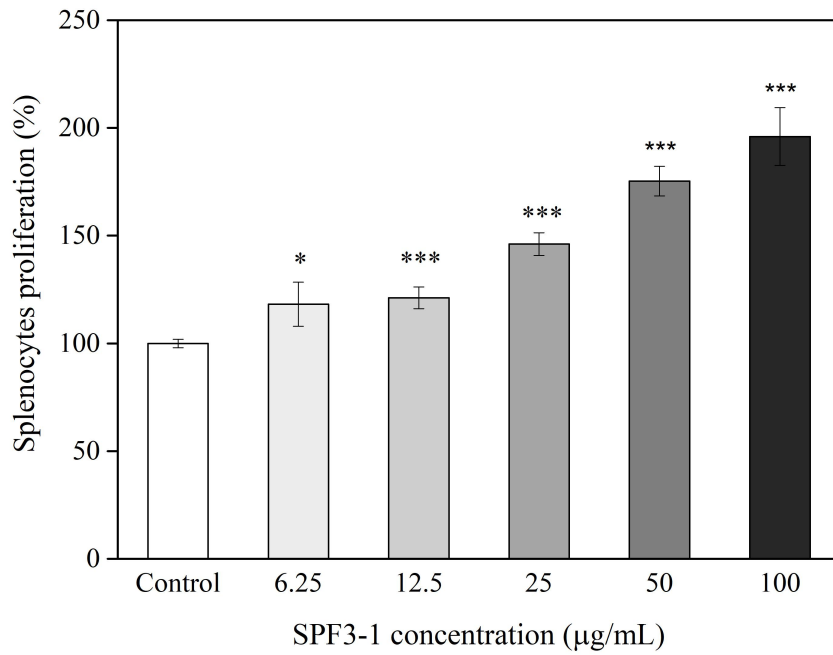


Figure 4- 5 Effect of SPF3-1 on splenocytes proliferation of 4T1-bearing mice

Results are represented as mean \pm SD ($n = 6$). NC: normal control, TC: tumor control. * $p < 0.05$, ** $p < 0.01$, and *** $p < 0.001$ denote statistically significant difference between the treated and control groups.

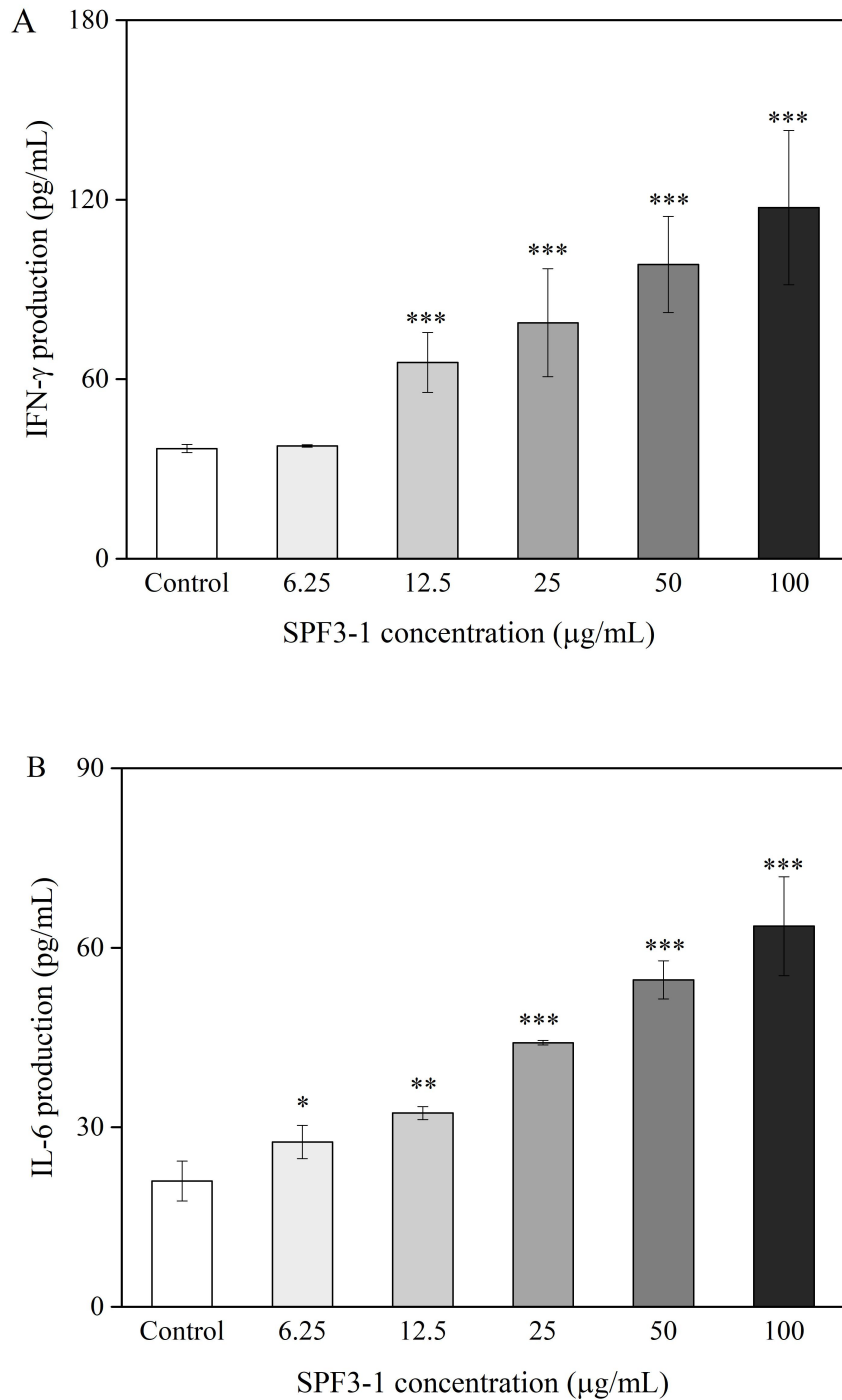


Figure 4-6 Effects of SPF3-1 on cytokines production in the culture medium of spleen lymphocytes

(A) IFN- γ generation; and (B) IL-6 level in culture medium. Results are represented as mean \pm SD ($n = 6$). NC: normal control, TC: tumor control. * $p < 0.05$, ** $p < 0.01$, and *** $p < 0.001$ denote statistically significant difference between the treated and control groups.

Chapter 5 Conclusions and perspectives

In this study, the crude polysaccharide HACP was extracted from *H. angustifolia*, the *in vivo* antioxidant and immunomodulatory activity of HACP was evaluated by using a 4T1 tumor-bearing mouse model. The major fractions of HACP were then separated and structure characterized. Moreover, the *in vitro* antioxidant and immunomodulatory activities of purified fractions were further evaluated and discussed.

5.1. Conclusions

The main conclusion of the work can be summarized as follows:

(1) HACP administration for 15 days significantly enhanced the mice serum antioxidant enzymes SOD and CAT activity, and increased immune cytokines TNF- α , IL-1 β , and IFN- γ by 3.43, 4.86 and 1.55-fold compared to the tumor control group. The increased antioxidant ability and immune response in mice resulted in reduced tumor size with inhibition rates of $34.58 \pm 10.20\%$, $57.80 \pm 8.65\%$ and $67.71 \pm 5.80\%$, respectively.

(2) Three major fractions were purified from HACP by using DEAE Sepharose Fast Flow and Sephacryl S-400 chromatography. SPF1-1, SPF2-1, and SPF3-1 are typical pectic polysaccharides which contain similar types of monosaccharide, while differ in their contents. The fraction SPF1-1 is mainly composed of glucose. The main neutral sugars of SPF2-1 are arabinose and glucose, and for SPF3-1 are rhamnose (Rha), arabinose (Ara) and galactose (Gal). The molecular weight of SPF1-1, SPF2-1, and SPF3-1 are 279 kD, 15.69 kD, and 13.36 kD, respectively.

(3) With highest inhibition rates against DPPH, ABTS, and superoxide radicals (74.59%, 57.4%, and 57.5%), and NO, and cytokines IL-6 production (10.40 μ M and 117.3 pg/mL), SPF3-1 was found to exhibit antioxidant and macrophages stimulation activity. And the significant efficiency antioxidant and immunomodulatory properties was found to highly correlated with its highest content of arabinose, galactose, xylose and uronic acid.

Taken together, results from this work revealed that polysaccharides from *H. angustifolia* possessed significant antioxidant and immunomodulatory activity both *in vitro* and *in vivo*, it can be used and developed as novel antioxidant and immunomodulatory therapeutics.

5.2. Future researches

Although polysaccharide SPF3-1 was detected to be effective in antioxidant and immune response *in vitro* conditions, its underlying molecular mechanisms and detailed

structure information still unclear. Therefore, bellow, further studies should be conducted.

(1) The repeating units, sugar sequence, and the degree of branching of SPFs need further research.

(2) The details on the mechanisms of SPF3-1 on macrophages would be the subject of continuing study.

(3) Further *in vivo* immunomodulatory identification of SPF3-1 are necessary.

References

- Aragon, F., Carino, S., Perdigon, G., & Moreno de LeBlanc, A. (2014). The administration of milk fermented by the probiotic *Lactobacillus casei* CRL 431 exerts an immunomodulatory effect against a breast tumour in a mouse model. *Immunobiology* **219**(6): 457-464.
- Baugh, J. A. & R. Bucala (2001). Mechanisms for modulating TNF alpha in immune and inflammatory disease *Current Opinion Drug Discovery & Development* **4**(5): 635-650.
- Berg, J. M., Tymoczko, J. L., & Stryer, L. (2012). *Biochemistry*. New York, NY: W.H. Freeman.
- Bitter & Muir (1962). A modified uronic acid carbazole reaction. *Analytical Biochemistry* **4**(4): 330-334.
- Chang, Y. S., Ku, Y. R., Lin, J. H., Lu, K. L., & Ho, L. K. (2001). Analysis of three lupane type triterpenoids in *Helicteres angustifolia* by highperformance liquid chromatography. *Journal of Pharmaceutical and Biomedical Analysis* **26**: 849-855.
- Chen, C. M., Chen, Z. T., & Hong, Y. L. (1990). A mansonone from *helicteres angustifolia*. *Phytochemistry* **29**(3): 980-982.
- Chen, W., Tang, W., Lou, L., & Zhao, W. (2006). Pregnane, coumarin and lupane derivatives and cytotoxic constituents from *Helicteres angustifolia*. *Phytochemistry* **67**(10): 1041-1047.
- Cheng, A. W., Wan, F. C., Wang, J. Q., Jin, Z. Y., & Xu, X. M. (2008). Macrophage immunomodulatory activity of polysaccharides isolated from *Glycyrrhiza uralensis* fish. *International Immunopharmacology* **8**: 43-50.
- Chidewe, C. K., Chirukamare, P., Nyanga, L. K., Zvidzai, C. J., & Chitindingu, K. (2016). Phytochemical Constituents and the Effect of Processing on Antioxidant Properties of Seeds of an Underutilized Wild Legume *Bauhinia Petersiana*. *Journal of Food Biochemistry* **40**(3): 326-334.
- Cho, W. C. S. & Leung, K. N. (2007). *In vitro* and *in vivo* anti-tumor effects of *Astragalus membranaceus*. *Cancer Letters* **252**(1): 43-54.
- Collins, A., Yuan, L., Kiefer, T. L., Cheng, Q., Lai, L., & Hill, S. M. (2003). Overexpression of the MT1 melatonin receptor in MCF-7 human breast cancer cells inhibits mammary tumor formation in nude mice. *Cancer Letters* **189**: 49-57.

- Cristina Diaz, A., Laura Espino, M., Arzoz, N. S., Maria Velurtas, S., Andrea Ponce, N. M., Stortz, C. A., et al. (2017). Free radical scavenging activity of extracts from seaweeds *Macrocystis pyrifera* and *Undaria pinnatifida*: Applications as functional food in the diet of prawn *Artemesia longinaris*. *Latin American Journal of Aquatic Research* **45**(1): 104-112.
- Debnath, T., Park,P.-J., Deb Nath, N. C., Samad, N. B., Park, H. W., & Lim, B. O. (2011). Antioxidant activity of *Gardenia jasminoides* Ellis fruit extracts. *Food Chemistry* **128**(3): 697-703.
- Di, T., Chen, G. J., Sun, Y., Ou, S. Y., Zeng, X. X., & Ye, H. (2017). Antioxidant and immunostimulating activities in vitro of sulfated polysaccharides isolated from *Gracilaria rubra*. *Journal of Functional Foods* **28**: 64-75.
- DuBois, M., Gilles, K., Hamilton, J., Rebers, P., & Smith, F. (1956). Colorimetric method for determination of sugars and related substances. *Analytical Chemistry* **28**(3): 350-356.
- Ferreira, S. S., Passos, C. P., Madureia, P., Vilnova, M., Coimbra, M. A. (2015). Structure-function relationships of immunostimulatory polysaccharides: A review. *Carbohydrate Polymers* **132**: 378-396.
- Ginsburg, O., Bray, F., Coleman, M. P., Vanderpuye, V., Eniu,A., Kotha, S. R., Sarker, M., Huong, T. T., & Conteh, L. (2017). The global burden of women's cancers: a grand challenge in global health. *The Lancet* **389**(10071): 847-860.
- Gnanasambanda, R. (2000). Determination of pectin degree of esterification by diffuse reflectance Fourier transform infrared spectroscopy. *Food Chemistry* **68**(3): 327-332.
- Gupta, R. K., Patel, A. K., Kumari, R., Chugh, S., Shrivastav, C., Mehra, S., & Sharma, A. N. (2012). Interactions between Oxidative Stress, Lipid Profile and Antioxidants in Breast Cancer: A Case Control Study. *Asian Pacific Journal of Cancer Prevention* **13**(12): 6295-6298.
- Harlev, E., Nevo, E., Lansky, E. P., Ofir, R., & Bishayee, A. (2012). Anticancer potential of aloes: Antioxidant, antiproliferative, and immunostimulatory attributes. *Planta Medica*, **78**(9):843–852.
- Hu, H., Liang, H. & Wu, Y. (2015). Isolation, purification and structural characterization of polysaccharide from *Acanthopanax brachypus*. *Carbohydrate Polymers* **127**: 94-100.

- Huang, C., Cao, X. Y., Chen, X. F., Fu, Y. P., Zhu, Y. G., Chen, Z. L., Luo, Q. H., Li, L. X., Song, X., Jia, R. Y., Yin, Z. Q., Feng, B., & Zou, Y. F. (2017). A pectic polysaccharide from *Ligusticum chuanxiong* promotes intestine antioxidant defense in aged mice. *Carbohydrate Polymers* **174**: 915-922.
- Huang, F., Zhang, R., Liu, Y., Xiao, J., Liu, L., Wei, Z., Yi, Y., Zhang M., & Liu, D. (2016). Dietary litchi pulp polysaccharides could enhance immunomodulatory and antioxidant effects in mice. *International Journal of Biological Macromolecules* **92**: 1067-1073.
- Huang, Q., Huang, R., Wei, L., Chen, Y., Lv, S., Liang, C., Zhang, X., Yin, F., Li, H., Zhuo, L., & Lin, X., (2013). Antiviral activity of methyl helicterate isolated from *Helicteres angustifolia* (Sterculiaceae) against hepatitis B virus. *Antiviral Research* **100**: 373-381.
- Jantan, I., Ahmad, W., & Bukhari, S. N. A. (2015). Plant-derived immunomodulators: an insight on their preclinical evaluation and clinical trials. *Frontiers in Plant Science* **6**.
- Jiang, C. X., Zhao, L., Li, S. L., Zhao, X. R., Zhang, Q. H., & Xiong, Q. P. (2013). Preliminary characterization and immunostimulatory activity of polysaccharides from *Glossaulax didyma*. *Food and Chemical Toxicology* **62**(1): 226-230.
- Jin, M., Huang, Q., Zhao, K., & Shang, P. (2013). Biological activities and potential health benefit effects of polysaccharides isolated from *Lycium barbarum* L. *International Journal of Biological Macromolecules* **54**: 16-23.
- Jin, M., Huang, Q., Zhao, K., & Shang, P. (2013). Biological activities and potential health benefit effects of polysaccharides isolated from *Lycium barbarum* L. *International Journal of Biological Macromolecules* **54**: 16–23.
- Klosterhoff, R. R., Bark, J. M., Glanzel, N. M., Iacomini, M., Martinez, G. R., Winnischofer, S. M. B., & Cordeiro, L. M. C. (2018). Structure and intracellular antioxidant activity of pectic polysaccharide from acerola (*Malpighia emarginata*). *International Journal of Biological Macromolecules* **106**: 473-480.
- Li, K., Lei, Z., Hu, X., Sun, S., Li, S., & Zhang, Z. (2015). *In vitro* and *in vivo* bioactivities of aqueous and ethanol extracts from *Helicteres angustifolia* L. root. *Journal of Ethnopharmacology* **172**: 61-69.
- Li, K., Yang, X., Hu, X., Han, C., Lei, Z., & Zhang, Z. (2016). *In vitro* antioxidant, immunomodulatory and anticancer activities of two fractions of aqueous extract from

- Helicteres angustifolia* L. root. *Journal of the Taiwan Institute of Chemical Engineers* **61**: 75-82.
- Li, S., Gao, A., Dong, S., Chen, Y., Sun, S., Lei, Z. & Zhang, Z. (2017). Purification, antitumor and immunomodulatory activity of polysaccharides from soybean residue fermented with *Morchella esculenta*. *International Journal of Biological Macromolecules* **96**: 26-34.
- Li, T., & Peng, T. (2013). Traditional Chinese herbal medicine as a source of molecules with antiviral activity. *Antiviral Research* **97**(1): 1-9.
- Li, Y., Xu, F., Zheng, M., Xi, X., Cui, X., & Han, C. (2018). Maca polysaccharides: A review of compositions, isolation, therapeutics and prospects. *International Journal of Biological Macromolecules* **111**: 894-902.
- Liu, J., Willfor, S., & Xu, C. (2015). A review of bioactive plant polysaccharides: Biological activities, functionalization, and biomedical applications. *Bioactive Carbohydrates and Dietary Fibre* **5**: 31-61.
- Liu, W., Wang, H., Yu, J., Liu, Y., Lu, W., Chai, Y., Liu, C., Pan, C., Yao, W., & Gao, X. (2016). Structure, chain conformation, and immunomodulatory activity of the polysaccharide purified from *Bacillus Calmette Guerin* formulation. *Carbohydrate Polymers* **150**: 149-158.
- Liu, X., Xie, J., Jia, S., Huang, L., Wang, Z., Li, C., & Xie, M. (2017). Immunomodulatory effects of an acetylated *Cyclocarya paliurus* polysaccharide on murine macrophages RAW264.7. *International Journal of Biological Macromolecules* **98**: 576-581.
- Liu, Y., Huang, G., & Hu, J. (2018). Extraction, characterisation and antioxidant activity of polysaccharides from Chinese watermelon. *International Journal of Biological Macromolecules* **111**: 1304-1307.
- Lo, T. C., Jiang, Y. H., Chao, A. L., & Chang, C. A. (2007). Use of statistical methods to find the polysaccharide structural characteristics and the relationships between monosaccharide composition ratio and macrophage stimulatory activity of regionally different strains of *Lentinula edodes*. *Analytic Chimica Acta* **584**(1): 50-56.
- Luo, K. W., Yue, G. G., Ko, C. H., Lee, J. K., Gao, S., Li, L. F., Li, G., Fung, K. P., Leung, P. C., & Lau, C. B. (2014). *In vivo* and *in vitro* anti-tumor and anti-metastasis effects of *Coriolus versicolor* aqueous extract on mouse mammary 4T1 carcinoma. *Phytomedicine* **21**: 1078-1087.

- Mao, G. H., Ren, Y., Feng, W. W., Li, Q., Wu, H. Y., Jin, D., Zhao, T. C. Q., Xu, L. Q., & Wu, X. Y. (2015). Antitumor and immunomodulatory activity of a water-soluble polysaccharide from *Grifola frondosa*. *Carbohydrate Polymers* **134**: 406-412.
- Meng, X., Liang, H., & Luo, L. (2016). Antitumor polysaccharides from mushrooms: a review on the structural characteristics, antitumor mechanisms and immunomodulating activities. *Carbohydrate Research* **424**: 30-41.
- Metcalf, N. B. & Alonso-Alvarez, C. (2010). Oxidative stress as a life-history constraint: the role of reactive oxygen species in shaping phenotypes from conception to death. *Functional Ecology* **24**(5): 984-996.
- Morgan, W. T. J. (1936). Studies in immuno-chemistry. I. The preparation and properties of a specific polysaccharide from *B. dysenteriae* (Shiga). *Biochemical Journal* **30**: 909-925.
- Murk, D. D., Silvestrini, B., & Cheng Y. (2002). Antioxidant superoxide dismutase-a review its function, regulation in the testis, and role in male fertility. *Contraception* **65**: 305-311.
- Nie, C., Zhu, P., Ma, S., Wang, M. & Hu, Y. (2018). Purification, characterization and immunomodulatory activity of polysaccharides from stem lettuce. *Carbohydrate Polymers* **188**: 236-242.
- Pan, H. H., Han, Y. Y., Huang, J. G., Yu, X. T., Jiao, C. W., Yang, X. B., Dhaliwal, P., Xie, Y. Z., & Yang, B. B. (2015). Purification and identification of a polysaccharide from medicinal *Amauroderma rude* with immunomodulatory activity and inhibitory effect on tumor growth. *Oncotarget* **10**(6): 17777-17791.
- Pan, M. H., Chen, C. M., Lee, S. W., and Chen, Z. T. (2008). Cytotoxic triterpenoids from the root bark of *Helicteres angustifolia*. *Chemistry & Biodiversity* 565-574.
- Ramberg, J. E., Nelson, E. D., & Sinnott, R. A. (2010). Immunomodulatory dietary polysaccharides: A systematic review of the literature. *Nutrition Journal* **9**: 54.
- Razali, F. N., Sinniah, S. K., Hussin, H., Zainal Abidin, N., & Shuib, A. S. (2016). Tumor suppression effect of *Solanum nigrum* polysaccharide fraction on Breast cancer via immunomodulation. *International Journal of Biological Macromolecules* **92**: 185-193.
- Ren, L., Perera, C., & Hemar, Y. (2012). Antitumor activity of mushroom polysaccharides: a review. *Food & Function* **3**(11): 1118-1130.

- Sarangarajan, R., Meera, S., Rukkumani, R., Sankar, P., & Anuradha, G. (2017). Antioxidants: Friend or foe? *Asian Pacific Journal of Tropical Medicine* **10**(12): 1111-1116.
- Schepetkin, I. A. & Quinn, M. T. (2006). Botanical polysaccharides: macrophage immunomodulation and therapeutic potential. *International Immunopharmacology* **6**(3): 317-333.
- Schepetkin, I. A., & Quinn, M. T. (2006). Botanical polysaccharides: Macrophage immunomodulation and therapeutic potential. *International Immunopharmacology* **6**: 317-333.
- Schepetkin, I. A., Faulkner, C. L., Nelson-Overton, L. K., Wiley, J. A., & Quinn, M. T. (2005). Macrophage immunomodulatory activity of polysaccharides isolated from *Juniperus scopolorum*. *International Immunopharmacology* **5**(13-14): 1783-1799.
- Shen, C. Y., Jiang, J. G., Li, M. Q., Zheng, C. Y., & Zhu, W. (2017). Structural characterization and immunomodulatory activity of novel polysaccharides from *Citrus aurantium* Linn. variant *amara* Engl. *Journal of Functional Foods* **35**: 352-362.
- Shen, H., Tang, G., Zeng, G., Yang, Y., Cai, X., Li, D., Liu, H., & Zhou, N. (2013). Purification and characterization of an antitumor polysaccharide from *Portulaca oleracea* L. *Carbohydrate Polymers* **93**(2): 395-400.
- Shi, L. (2016). Bioactivities, isolation and purification methods of polysaccharides from natural products: A review. *International Journal of Biological Macromolecules* **92**:37-48.
- Siu, K. C., Xu, L., Chen, X., & Wu, J. Y. (2016). Molecular properties and antioxidant activities of polysaccharides isolated from alkaline extract of wild *Armillaria ostoyae* mushrooms. *Carbohydrate Polymers* **137**: 739-746.
- Smirnoff, N., Cumbes, Q.J., 1989. Hydroxyl radical scavenging activity of compatible solutes. *Phytochemistry* **28**: 1057-1060.
- Sun, H., Zhang, J., Chen, F., Chen, X., Zhou, Z., & Wang, H. (2015). Activation of RAW264.7 macrophages by the polysaccharide from the roots of *Actinidia eriantha* and its molecular mechanisms. *Carbohydrate Polymers* **121**: 388-402.
- Sun, X., Gao, R. L., Xiong, Y. K., Huang, Q. C. & Xu, M. (2014). Antitumor and immunomodulatory effects of a water-soluble polysaccharide from *Lilii Bulbus* in mice. *Carbohydrate Polymers* **102**: 543-549.

- Sun, Y., S. Hou, S., Song, B., Zhang, C., Ai, X., & Liu, N. (2018). Impact of acidic, water and alkaline extraction on structural features, antioxidant activities of *Laminaria japonica* polysaccharides. *International Journal of Biological Macromolecules* **112**:985-995.
- Tang, W., Hemm, I., & Bertram, B. (2003a). Recent development of antitumor agents from Chinese herbal medicines. Part II. High molecular compounds(3). *Planta Medica* **69**(3): 193-201.
- Tao, K., Fang, M., Alroy, J., & Sahagian, G. G. (2008). Imagable 4T1 model for the study of late stage breast cancer. *BMC Cancer* **8**: 228.
- Telo, S., Halifeoglu, I., & Ozercan, I. H. (2017). Effects of stinging nettle (*Urtica Dioica* L.) on antioxidant enzyme activities in rat model of mammary gland cancer 164-170. *Iranian Journal of Pharmaceutical Research* **16**: 164-170.
- Tian, L., Zhao, Y., Guo, C., & Yang, X. (2011). A comparative study on the antioxidant activities of an acidic polysaccharide and various solvent extracts derived from herbal *Houttuynia cordata*. *Carbohydrate Polymers* **83**(2): 537–544.
- Tu, J., Sun, H. X., & Ye, Y. P. (2008). Immunomodulatory and antitumor activity of triterpenoid fractions from the rhizomes of *Astilbe chinensis*. *Journal of Ethnopharmacology* **119**(2): 266-271.
- Vijayarathna, S., & Sasidharan, S. (2012). Cytotoxicity of methanol extracts of *Elaeis guineensis* on MCF-7 and Vero cell lines. *Asian Pacific Journal of Tropical Biomedicine* **2**(10): 826-829.
- Wang M, & Liu, W.(1987). A naphthoquinone from *Helicteres angustifolia*. *Phytochemistry* **26**: 578-579.
- Wang, C., Feng, L., Su, J., Cui, L., Dan, L., Yan, J., Ding, C., Tan X., & Jia, X. (2017). Polysaccharides from *Epimedium koreanum* Nakai with immunomodulatory activity and inhibitory effect on tumor growth in LLC-bearing mice. *Journal of Ethnopharmacology* **207**: 8-18.
- Wang, G. C., T. Li, Y. R. Wei, Y. B. Zhang, Y. L. Li, S. C. Sze and W. C. Ye (2012). Two pregnane derivatives and a quinolone alkaloid from *Helicteres angustifolia*. *Fitoterapia* **83**(8): 1643-1647.
- Wang, H., Liu, Y. M., Qi, Z. M., Wang, S. Y., Liu, S. X., Li, X., et al. (2013). An overview on natural polysaccharides with antioxidant properties. *Current Medicinal Chemistry*, **20**(23): 2899-2913.

- Wang, J., Hu, S., Nie, S., Yu, Q., & Xie, M. (2016). Reviews on mechanisms of *in vitro* antioxidant activity of polysaccharides. *Oxidative Medicine and Cellular Longevity* **2016**: 5692852.
- Wang, W., Zou, Y., Li, Q., Mao, R., Shao, X., Jin, D., Zheng, D., Zhao, T., Zhu, H., Zhang, L., Yang, L., & Wu, X. (2016). Immunomodulatory effects of a polysaccharide purified from *Lepidium meyenii* Walp. on macrophages. *Process Biochemistry* **51**(4): 542-553.
- Wang, X., Chen, Q., & Lü, X. (2014). Pectin extracted from apple pomace and citrus peel by subcritical water. *Food Hydrocolloids* **38**: 129-137.
- Wang, Y., Huang, M., Sun, R., & Pan, L. (2015). Extraction, characterization of a Ginseng fruits polysaccharide and its immune modulating activities in rats with Lewis lung carcinoma. *Carbohydrate Polymers* **127**: 215-221.
- Wang, Z., Xie, J., Yang, Y., Zhang, F., Wang, S., Wu, T., et al. (2017). Sulfated *Cyclocarya paliurus* polysaccharides markedly attenuates inflammation and oxidative damage in lipopolysaccharide-treated macrophage cells and mice. *Scientific Reports* **7**: 40402.
- Wei, C. Y., He, P. F., He, L., Ye, Q. Q., Cheng, J. W., Wang, Y. B., Li, W. Q., & Liu, Y. (2017). Structure characterization and biological activities of a pectic polysaccharide from cupule of *Castanea henryi*. *International Journal of Biological Macromolecules* **8**: 35-42.
- Xu, H., Yao, L., Sun, H., & Wu, Y. (2009). Chemical composition and antitumor activity of different polysaccharides from the roots of *Actinidia eriantha*. *Carbohydrate Polymers* **78**(2): 316-322.
- Yu, X. H., Liu, Y., Wu, X. L., Liu, L. Z., Fu, W., & Song, D. D. (2017). Isolation, purification, characterization and immunostimulatory activity of polysaccharides derived from American ginseng. *Carbohydrate Polymers* **156**: 9-18.
- Yu, Y., Shen, M., Song, Q. & Xie, J. (2018). Biological activities and pharmaceutical applications of polysaccharide from natural resources: A review. *Carbohydrate Polymers* **183**: 91-101.
- Yu, Y., Shen, M., Wang, Z., Wang, Y., Xie, M., & Xie, J. (2017). Sulfated polysaccharide from *Cyclocarya paliurus* enhances the immunomodulatory activity of macrophages. *Carbohydrate Polymers* **174**: 669-676.

- Zeng, W.-C., Sun, Q., Zhang, W.-H., Liao, X.-P., & Shi, B. (2017). Antioxidant activity in vivo and biological safety evaluation of a novel antioxidant peptide from bovine hair hydrolysates. *Process Biochemistry* **56**: 193-198.
- Zhang, C. H., Yu, Y., Liang, Y. Z., & Chen, X. Q. (2015). Purification, partial characterization and antioxidant activity of polysaccharides from *Glycyrrhiza uralensis*. *International Journal of Biological Macromolecules* **79**: 681-686.
- Zhang, J., Sun, R., Wei, H., & Tian, Z. (2005). Antitumor effects of recombinant human prolactin in human adenocarcinoma-bearing SCID mice with human NK cell xenograft. *International Immunopharmacology* **5**(2): 417-425.
- Zhang, L., Hu, Y., Duan, X., Tang, T., Shen, Y., Hu, B., Liu, A., Chen, H., Li, C., & Liu, Y. (2018). Characterization and antioxidant activities of polysaccharides from thirteen boletus mushrooms. *International Journal of Biological Macromolecules* **113**: 1-7.
- Zhang, M. M., Wang, G., Lai, F. R., & Wu, H. Structural Characterization and Immunomodulatory Activity of a Novel Polysaccharide from *Lepidium meyenii*. *Journal of Agriculture and Food Chemistry* 1921-1931.
- Zhang, S., Nie, S., Huang, D., Li, W., & Xie, M. (2013). Immunomodulatory effect of *Ganoderma atrum* polysaccharide on CT26 tumor-bearing mice. *Food & Chemistry* **136**(3-4): 1213-1219.
- Zhang, S., Shao, Q. Q., Shen, Z. H., & Su, S. K. (2017). Immunomodulatory response of 4t1 murine breast cancer model to camellia royal jelly. *Biomedical Research* **28**(3): 1223-1230.
- Zhang, S., Wang, Q., Li, W. F., Wang, H. Y., & Zhang, H. J. (2004). Enhanced antitumor immunity by murine cytokine activated T lymphocytes after cocultured with bone marrow derived dendritic cells pulsed with whole tumor lysates. *Leukemia Research* **28**(10): 1085-1088.
- Zhao, J., Zhang, F., Liu, X., St Ange, K., Zhang, A., Li, Q., & Linhardt, R. J. (2017). Isolation of a lectin binding rhamnogalacturonan-I containing pectic polysaccharide from pumpkin. *Carbohydrate Polymers* **163**: 330-336.
- Zhu, L., Cao, J., Chen, G., Xu, Y., Lu, J., Fang, F., & Chen, K. (2016). Anti-tumor and immunomodulatory activities of an exopolysaccharide from *Rhizopus nigricans* on CT26 tumor-bearing mice. *International Immunopharmacology* **36**: 218-224.

Acknowledgements

I wish to express my sincere appreciation to my principal advisor, Professor Zhenya Zhang, for his kindly and warmly guidance and encouragement.

I also would like to express my great appreciation to my dissertation committee members, Professor Zhongfang Lei, Professor Kazuya Shimizu, and Professor Hideaki Maseda for their numerous suggestions, comments, willingness and helpful discussions to serve as my advisory committee members.

I would also like to thank all of my friends in the laboratory for their friendship and contributions. I wish to express my appreciation to Miss Xi Yang, Mr. Long Xiao, and Mr. Yuepeng Wang, for their countless assistance during the years of my study here.